ETH
Eidgenössische Technische Hochschule Zürich
Swiss Federal Institute of Technology Zurich

A / S Architecture and Building Systems

Daniel Weber
BSc Mechanical Engineering

Modelling building thermal systems to investigate energy and comfort dependent control strategies

Master Thesis

ITA – Architecture and Building Systems
Swiss Federal Institute of Technology (ETH) Zurich

Examiner:
Prof. Dr. Arno Schlüter

Supervisor:
Gearóid Lydon

Zurich, October 16, 2018

Abstract

In this thesis, a model of the thermal energy systems of the NEST HiLo building is created through combination of three software programs. TRNSYS is responsible for general building thermal calculations and acts as a bridge between MATLAB and CONTAM. The latter is used to model natural and mechanical ventilation systems and the general interzonal air flows. MATLAB is used to implement a customised TABS (thermally active building system) model to fit the non-typical lightweight structural elements of the funicular floor and the thin shell roof. Additionally, it is used to enable a gateway for control inputs to the whole building model. Vertical and horizontal resolution simplifications for MATLAB's TABS model are presented, where the former is found to be justified, as computation time is saved and loss of precision is negligible. For the latter, no absolute conclusion can be drawn, as precision loss is bigger and justification depends on the users preferences on the models level of detail. First test simulations show expected results on interaction between the systems.

Acknowledgements

By doing this master's thesis, I could greatly expand my knowledge about building simulations and the workings of RC models. I have found interest in a specific topic, I only had sparse experience in before. Using my knowledge gained in the past years and being able to apply it in a project where I could put 100% of my energy into, was a satisfying and complementing finale to my studies.

The depth and quality of this thesis would not have been possible without the help and competence of some special people. I would like to thank Markus Koschenz and Beat Lehmann for taking the time and interest to review the modified TABS model and sharing their valuable expertise on this matter.

Thank you Stuart W. Dols for helping a great deal in modelling the ventilation systems in CONTAM.

Additionally, thank you Christian Scheidegger and Eloise Sok from Saint-Gobain for supplying HiLo's glazing tinting states in TRNSYS' library format.

Furthermore, many thanks to Prof. Dr. Arno Schlueter for accepting me into his group and Dr. Johannes Hofer for giving me feedback up to my interim presentation.

Also, I would like to appreciate Antonia Weber's help in proof reading the thesis and thereby giving sophisticated grammatical inputs.

Last but surely not least, I want to thank my supervisor Gearóid Lydon for always giving me great advice and supporting me in all matters whatsoever. You were always very understanding and successfully guided me through the last six months.

Contents

List of Acronyms

AHU	Air Handling Unit
BA	Building Automation
BRG	Block Research Group
CFD	Computational Fluid Dynamics
CHTC	Convective Heat Transfer Coefficient
DG	Distributed Generation
EPS	Expanded Polystyrene
EU	European Union
GHG	Greenhouse Gases
HiLo	High Performance, Low Energy
HC	Heating Curve
HVAC	Heating Ventilation and Air Conditioning
IEA	International Energy Agency
IAQ	Indoor Air Quality
IRA	Integrated Room Automation
MPC	Model Predictive Control
NEST	Next Evolution in Building Systems
NRPE	Non-Renewable Primary Energy
NZEB	Net Zero Energy Building
PB	Performance Bound
RC	Resistor-Capacitor
RBC	Rule Based Control
SMPC	Stochastic Model Predictive Control
TABS	Thermally Activated Building System

List of Figures

Introduction

1.1 Motivation

The world's climate is changing. Since the 1950s, carbon dioxide levels in the atmosphere have risen above 300 ppm. The probability of this change being anthropogenic is 95% [3]. Mankind alone is responsible to mitigate this effect in order to avoid more extreme catastrophic climate events in the future and negative impacts on our ecosystem. In order to manage global warming impacts, reducing greenhouse gases (GHG) has been identified as a key metric to track improvements [4].

The European Union (EU) has set targets for 2050 to reduce GHG levels by 80% of the 1990 levels [5]. To reach this goal, energy usage coming from burning fossil fuels has to be reduced, since it is the largest source of GHG emissions [6]. The International Energy Agency (IEA) states that the building sector is the biggest energy-consuming sector, accounting for over one-third of final energy consumption globally and an equally important source of CO_2 emissions [7]. Therefore, it is an area with high potential for reduction of GHG emissions.

Article 9 of Directive 2010/31/EU states that all buildings built after 2020 have to be Net Zero Energy Buildings (NZEB) [8]. Additionally, 20% of final energy consumption has to stem from renewable energy sources, which is included in the 2009 Renewable Energy Sources Directive 2009/28/EC [9]. Consequently, on site renewable energy generation, for example solar collectors, photovoltaics or geothermal heat pumps, will have to be included in new buildings. Distributed generation (DG) also positively affects the electricity grid, if the generated DC power, for example from photovoltaics, is consumed directly on site or stored in a battery and is not fed into the grid. Furthermore, by bypassing the DC-AC (into the grid) and later the AC-DC (from the grid) conversions, energy losses are minimised and efficiency is increased.

In the building sector, there are different fields for potentially reducing energy consumption. One is the widely known approach of reducing operational energy during the usage of a building. A staggering 76% of operational energy in commercial and residential buildings is related to keeping specific thermal comfort levels, which is summarised as heating ventilation and air conditioning (HVAC) [10].

Embodied energy is another field with promising energy reduction potential, which is not yet as popular as the latter. It describes the energy consumed by all of the processes associated with the production of a product. For example in case of a building, it spans from mining and processing of natural resources to manufacturing, transport and product delivery [11]. Its share of total energy for buildings can range from 9% to 46% [9][12].

One way to achieve energy savings is to combine reductions in both operational and embodied energy in multi-functional building elements. Such elements can carry out structural, architectural and energy system functions at the same time [2].

The aforementioned multi-functional building elements along with other innovations will be realised in the HiLo (High performance, Low energy) building. HiLo is developed by Architecture and Building Systems and the Block Research Group (BRG) from the Institute of Technology in Architecture, ETH Zürich.

In this thesis, the modelling and simulation of thermal components of HiLo is completed using the building software TRNSYS [13]. The thermal components include a hydronic radiant heating and cooling system embedded in both a lightweight funicular floor and a thin shell roof, which are thermally active building systems (TABS), and are coupled with natural and mechanical ventilation systems to further improve the efficiency of the whole HVAC system. Additionally, electrochromic glass will be implemented to control solar gains and lighting levels in the unit. The components interaction with each other will be analysed in a first night cooling test case.

One of TRNSYS' advantages is its versatility of calling other applications. This allows specific thermal systems to be modelled in other software in order to exploit their sophisticated detailed calculations and achieve an overall more precise model. In this case, HiLo's TABS will be modelled in MATLAB [14], its ventilation system in CONTAM [15] and the electrochromic glass in TRNBuild, TRNSYS' 3D multizone building component. Furthermore, MATLAB will be used as a gateway for all control inputs going into the simulation.

This thesis supplies a thermal model of HiLo, which can later be used for its whole building simulation with respect to energy efficiency and occupancy comfort using an integrated room automation (IRA) apporach, that deals with the combined control of such systems [16]. The end goal is to investigate the optimum setup of TRNSYS, MATLAB and CONTAM to match the research questions of the thermal systems and define a first set of control templates for when HiLo comes alive in 2019.

1.2 Literature Review

A complete and detailed list of HiLo's innovations can be found in [17]. Note that for this thesis only the thermal components, which are presented below, will be relevant, as is discussed in Section 1.1.

TABS in HiLo are the result of combining a lightweight funicular floor and a thin shell roof with a hydronic radiant and cooling system. In principal, they are pipes

carrying heating or cooling fluid (usually water) embedded in a concrete slab. The massive structure of such a slab acts as a thermal sink, as its large heat capacity is exploited. Consequently, TABS have a slow thermal inertia, which can act as a buffer mechanism for diurnal changes. Thus, heat or cold is released with a certain delay to the room [16]. Another advantage of TABS are their large surface area. This means that supply water temperatures can be near room temperature, making it a low exergy system [2].

The aforementioned characteristics have the downside of needing sophisticated control mechanisms, as room temperatures can only react very slowly to setpoint changes. Additionally, situations with different comfort requirements in different rooms but with the same water supply are a realistic scenario and even more difficult to achieve. Conventional control concepts are usually rule based control (RBC) and are established on the supply water temperature depending on the outside temperature through a heating curve (HC), where internal gains are neglected. The cooling mode is usually constant temperature derived from the maximum load in the system [18].

Oldewurtel compared the strategies RBC, model predictive control (MPC) and stochastic model predictive control (SMPC) to a performance bound (PB) benchmark "in a large scale simulation study for a large number of different cases varying in the building type, HVAC system, and weather conditions" in [19]. It was concluded that SMPC outperformed RBC with respect to "non-renewable primary energy (NRPE) usage, thermal comfort statistics and advantageous room temperature dynamics". When comparing SMPC to MPC, the added stochastic part resulted in SMPC being "superior both in terms of NRPE usage and comfort violations", as the uncertainty of the weather forecast was accounted for in its control decisions.

Natural and mechanical ventilation supports the hydronic radiant and cooling system to increase its efficiency and is also responsible for indoor air quality (IAQ) in HiLo. The difference between them is that the former uses no additional power whereas the latter does in order to reach the shared goal of exchanging used indoor with fresh outdoor air. Therefore, natural ventilation is the preferred method as it saves energy and its potential should be maximized [20].

Natural ventilation uses pressure differences, which are caused by buoyancy or wind forces, to create a natural flow of air [21]. There are two types of wind driven natural ventilation. Firstly, there is cross ventilation, in which a building has openings on different sides. Any wind will then lead to a pressure difference between the sides and an air flow between the openings is created. The second method is single-sided ventilation, in which openings for the ventilation are on the same building side. It is less effective than cross ventilation and mostly used in cases where it is the only natural ventilation possibility [22].

Buoyancy-driven ventilation is based on the principle that a fluid with smaller density rises in a fluid with higher density, which is also known as stack effect. Density differences can be achieved, for example, through a temperature differential between inside and outside air of a building. If there is a lower and upper aperture present, an upflow air

displacement can be achieved [23].

There are multiple types of mechanical ventilation systems. The simplest method is air circulation with the help of a fan, where no air exchange with the outside is happening. Another type is a pressure system, which blows fresh outside air into the building. It leads to a higher inside pressure compared to outside and an air flow is achieved. A vacuum system does the opposite by sucking air out of the building, therefore creating lower pressure inside. Combining the former two systems results in a balanced system. Fresh air is getting blown in and used air is getting sucked outside the building. It leads to similar pressure inside as outside, which gives way to less air infiltration and draughts. Another type is a local exhaust system, which ventilates a specific spot in the building, for example, a cooker hood. As soon as outside air is included in ventilating a building, it can strongly influence inside temperatures. To counteract this effect, a heat recovery system can be integrated, which uses the heat of the exiting air in a heat exchanger to warm up the incoming colder outside air [24].

Hybrid ventilation is the combination of natural and mechanical ventilation, also known as mixed-mode ventilation [25]. It comes into play when natural ventilation alone does not meet the necessary air exchange needs and exploits the advantages of energy-free natural ventilation in addition with a higher level of control from mechanical ventilation [26].

Electrochromic glass will be integrated in the south and west facing facades of HiLo and will be used to control solar gains into the main living area. It functions by applying voltage to the glass leading to a change in its optical properties [27]. Therefore, it is possible to control light and heat flows through windows. Specifically, absorbtance, reflectance or scattering of light can be influenced [28]. There are different positive aspects to electrochromic glass, which are that "(1) they only require power during switching, (2) they have a long-term memory (12 - 48 h), (3) they require a small voltage to switch (1 - 5 V), (4) they are specular in all states and (5) they have potential for large-area fabrication" [29].

Compared to normal windows, electrochromic glass can achieve energy savings of up to 30% by decreasing the need for space cooling [28]. Furthermore, it outperforms traditional external shading devices such as overhangs and fins in terms of energy efficiency [30].

1.3 Problem Statement

Complex interactions are happening between HiLo's codependent thermal systems. Slow acting TABS with large thermal masses make it difficult to use a simple RBC approach. A more sophisticated control algorithm needs to be implemented to set correct inputs in advance. This requires a robust thermal model of HiLo to simulate its behavior in the near term future to increase energy efficiency and guarantee occupancy comfort throughout its operation.

1.4 Objectives

Based on the problem statement, the objectives in this thesis are as follows.

1. Establishing an interconnection between MATLAB, TRNSYS and CONTAM
2. Modelling of HiLo's thermal components and connecting them through TRNSYS including:
    - TABS in thin shell roof and funicular floor structures (MATLAB)
    - Natural and mechanical ventilation (CONTAM)
    - Electrochromic glass (TRNBuild)
3. Conducting a first simple test case simulation of HiLo's full thermal model to verify the working interaction between the different components in their software programs

Methodology

In this chapter, methods are presented of how three different software programs are combined and a TABS model is created for HiLo's building simulation.

2.1 Interconnectivity concept of MATLAB, CONTAM and TRNSYS

TRNSYS' strength lies in its versatility to include other software programs in its calculations. Thus, it is possible to use separate programs in combination that serve their specific purpose in building simulations. CONTAM is such a program, which enables sophisticated airflow calculations [15]. Coupled with TRNBuild, the 3D multizone building component of TRNSYS, it can enable the creation of powerful building models. By adding MATLAB to the mix, a gateway for control inputs is supplied. Additionally, MATLAB enables the option of including a TABS RC model tailored to HiLo's exotic specifications, which would not be possible with the standard TABS model from TRNBuild at the same level of precision, explained later in Section 2.2.1.

The interconnectivity of the three software programs is shown in Figure 2.1. Their interaction with one another can be presented as follows. CONTAM measures CO_2 values through sensors and sends them to the ventilation control unit in MATLAB. The controller decides, for example, to open windows or start mechanical ventilation. These inputs are sent back to CONTAM, where they are executed. CONTAM calculates airflows and sends them to TRNBuild, where thermal calculations happen. In exchange, CONTAM receives air temperatures from TRNBuild.

HiLo's electrochromic glass also has a controller in MATLAB, which receives temperatures and solar radiation to decide whether to darken or brighten the windows' glazing. An input is sent to TRNBuild where a window ID is chosen, which corresponds to the tinting state that affects the glazing's g-value. Hence, solar gains can be controlled into the building.

The tailored TABS model in MATLAB receives heat fluxes to its surfaces, calculates their temperatures and then sends them back to TRNBuild. The TABS controller decides, for example, to adjust supply water mass flow and temperature.

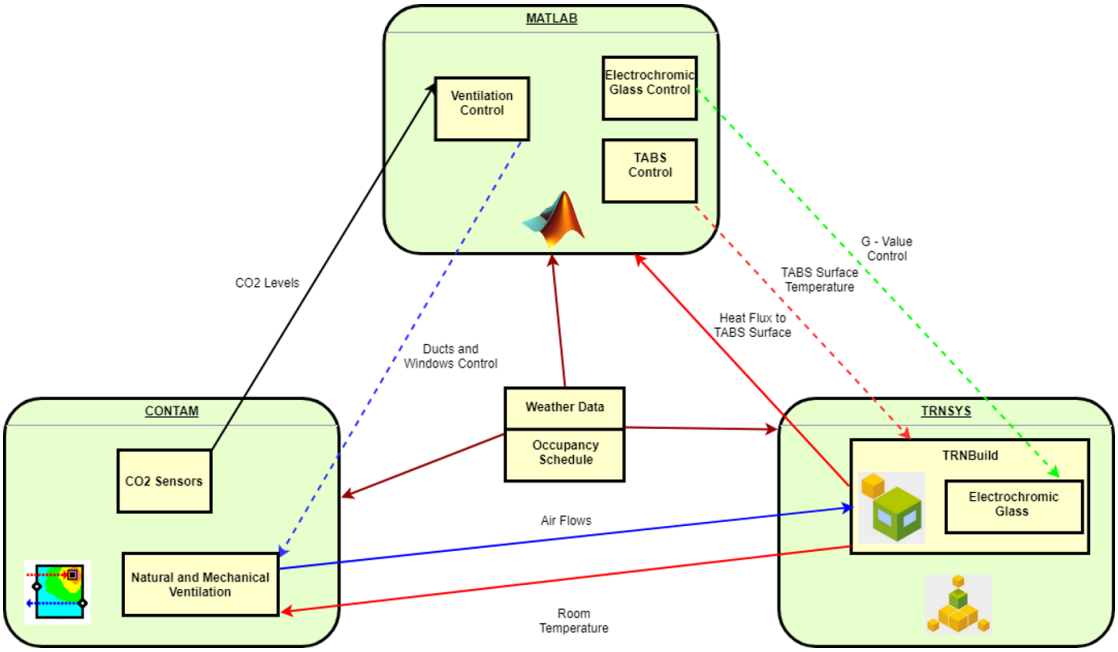

Figure 2.1: Interconnectivity concept of MATLAB, TRNSYS and CONTAM.

Weather data and occupancy schedule are the same for all three software programs. It has to be noted, that the sketch does not quite capture the exact flows of the signals, in order to keep a clear and easily understandable picture. For example, weather data actually stems from TRNSYS and is distributed to MATLAB and CONTAM. Occupancy schedule is read in through MATLAB where heat and CO_2 gains are directly calculated and sent to TRNSYS and CONTAM. Also, there is no direct connection between MATLAB and CONTAM. Every exchange between these two programs happens through TRNSYS, which acts in a sense as a bridge.

2.2 TABS RC Model

A standard TABS RC model from Tödtli et al [1] is taken and adjusted to capture the geometry of HiLo's TABS. Their model includes TABS in a whole RC building model. The specific structure with its temperature nodes and resistance as well as capacitance values is shown in Figure 2.2. For our purpose, only the part in the red rectangular is necessary, which spans from supply water temperature to surface temperatures and is presented in the following sections. TRNBuild is used to simulate the rest of the building.

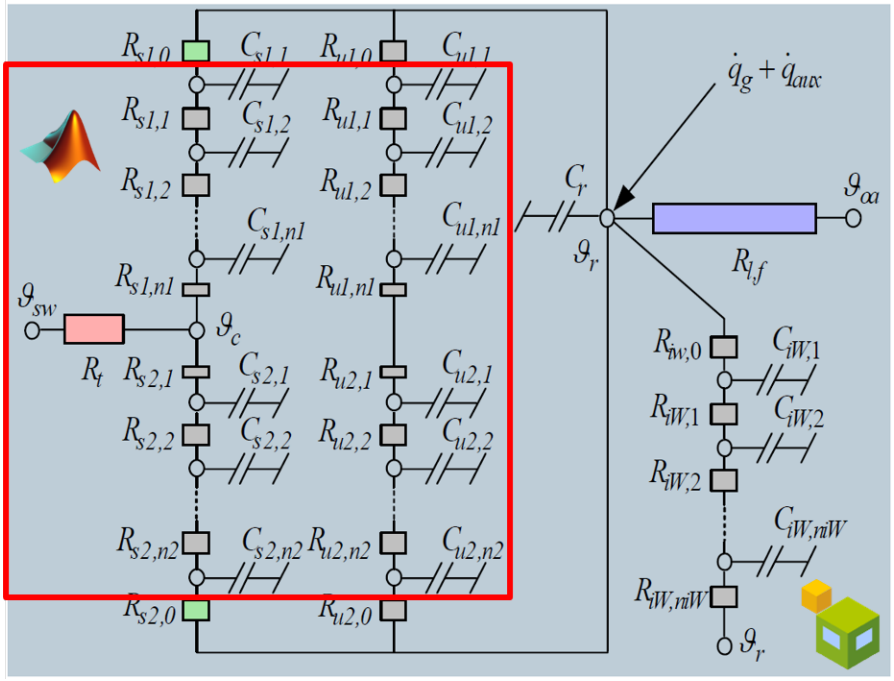

Figure 2.2: RC model of complete building including TABS, which are marked in red and modelled in MATLAB and the rest in TRNBuild, which includes building envelope, inside walls, building and auxiliary heat gains [1].

It must be noted, that the model is partly adjusted in its horizontal plane with the capillary mats model from Koschenz and Lehmann presented in [31]. This is due to the fact that a necessary boundary condition required for standard TABS cannot be met, which is shown in (2.1).

$$\frac{d_i}{d_x} > 0.3 \qquad i = 1, 2 \tag{2.1}$$

Denominator d_x is pipe spacing and numerator d_i is layer thickness. Numbers 1 and 2 depict the two layers adjacent to the pipe, where the top layer in HiLo's TABS is too thin that it could lead to realistic results.

2.2.1 Capturing HiLo TABS Geometry

HiLo's floor TABS are made up of a concrete vault with fins, where an expanded polysterene (EPS) filling sits in-between them, shown in Figure 2.3. It supports structural and thermal processes and makes it a lightweight system.

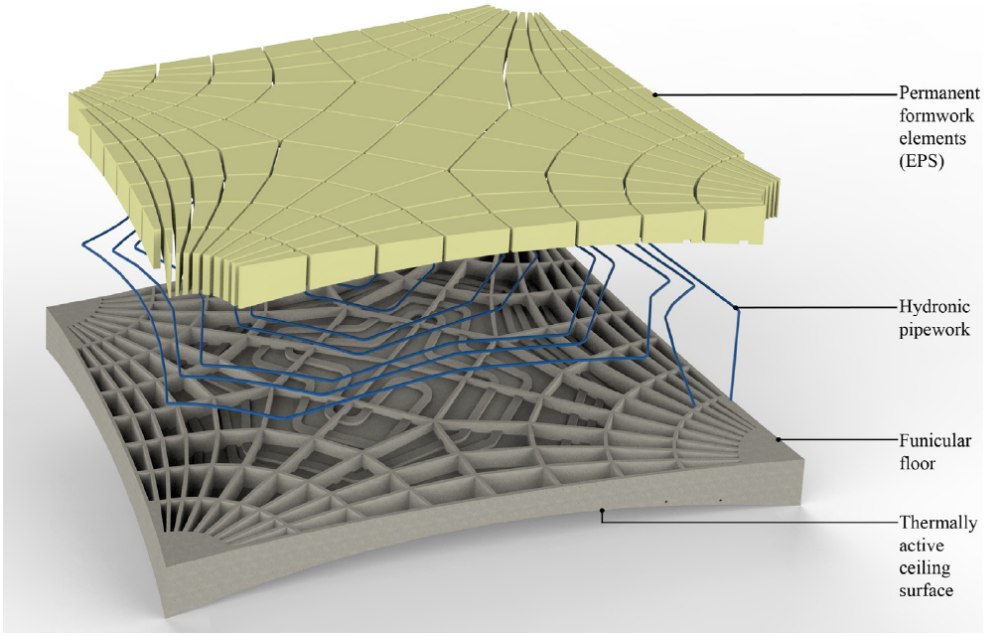

Figure 2.3: Structure of concrete funicular floor TABS with vertical fins and EPS filling in between. The hydronic pipe work and its spirale configuration is shown in blue [2].

As the vault has a funicular shape, its thickness changes throughout. Additionally, tension forces are resolved at the perimeter of the structure, due to the curvature of the vault, and thicknesses of vault and fins of 20 mm are possible [2].

The roof TABS' differences to the floor TABS are the non existent vertical concrete fins and the layer configuration. However, the changing thickness within one of its layers is present, too. In order to use a general model for vertical layer configuration in both roof and floor TABS, the concrete fins between the EPS insulation in HiLo's floor TABS can be included by using an averaged EPS-concrete layer.

Additionally, pipe layout is in spiral form, where the pipe starts at the outside, circles into the middle where it turns around and circles out again. Because of this and the varying thickness of HiLo's TABS, the standard model in TRNBuild is assumed to not be sufficient and a specially tailored version is created as follows.

From here on forth, HiLo's floor TABS will be used to present the general RC model for both systems. Slight differences between the two are mentioned throughout the sections. First, the TABS model is cut into pieces, as shown in Figure 2.4.

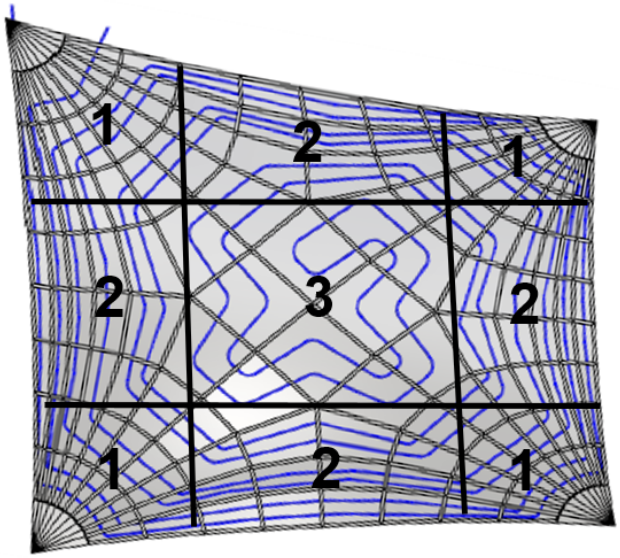

Figure 2.4: Top view of floor TABS with its pipe configuration and division into pieces with different geometrical properties.

The ones with similar geometry are grouped together into subsections. In Figure 2.5, pieces of the same number create three different subsections, where it is now possible to vary parameters such as floor area A_{fl}, activated floor area A_{ta}, pipe length l and layer thickness d_y.

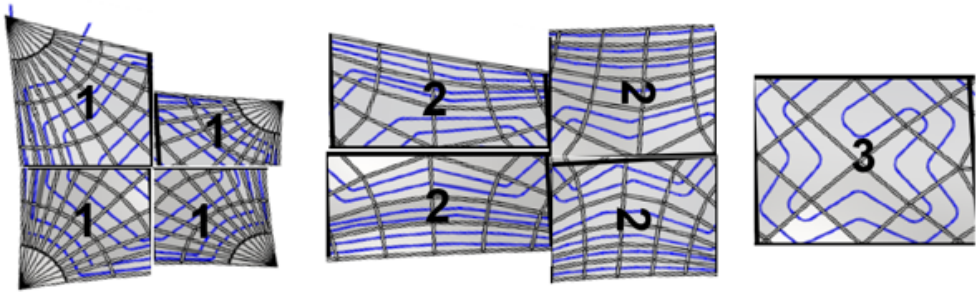

Figure 2.5: Top view of floor TABS cut and regrouped into subsections with similar geometrical properties.

A first assumption is, that for all subsections a uniform mean water temperature is used, which is due to the pipe spiral configuration. In subsection 3 Figure 2.5, where the pipe turns around, the midpoint of the pipe is assumed. Additionally, by assuming a linear temperature drop, the temperature at this point is the average of supply water and return water temperature, from now on called mean water temperature $\bar{\theta}_w$. Furthermore, by looking closely at the pipe configuration in Figure 2.5, it is visible that there are always two pipes next to each other, where one carries supply water and the other return water.

Consequently, the temperatures of both pipes average themselves out to mean water temperature, found at the midpoint of the pipe.

The TABS' pipes are placed on a concrete layer and have another thin concrete layer sheathed around them, presented in Figure 2.6 on the left.

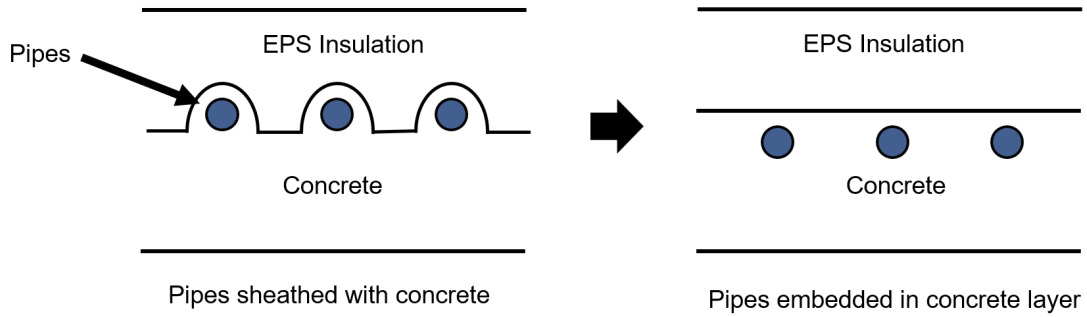

Figure 2.6: Side view of simplification process of pipe adjacent layers in floor TABS.

To fit the RC model, a simplification is made as follows. The pipes are slightly pushed down into the lower concrete layer, whereas the top sheathing is leveled to a straight plane, shown in Figure 2.6 on the right. Hence, the configuration is ready to be represented by the RC model.

2.2.2 Supply Water Temperature to Core Temperature

In this and the following few sections, the differences of the RC model from [1], with the adjustment for capillary mats from [31], and the modified model for HiLo are presented. A full model description with all mathematical calculations can be found in the two cited sources. A first adjustment is made from supply water temperature θ_{sw} to core temperature θ_{core}. The standard model is shown in Figure 2.7.

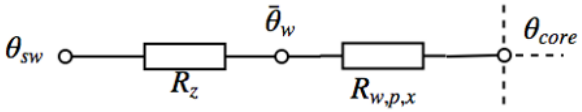

Figure 2.7: Standard TABS RC part from supply water temperature to core temperature.

From θ_{sw} thermal energy goes through resistance R_z, in the water along the pipe in z-direction, and reaches mean water temperature $\bar{\theta}_w$. From here, located in the circular middle of the pipe, the connection is made to core temperature θ_{core} over the three resistances summed up as $R_{w,p,x}$, which depict water, pipe wall and slab resistance in x-direction.

At $\bar{\theta}_w$, HiLo's TABS split into three parallel branches, shown in Figure 2.7, that represent the subsections presented in Section 2.2.1.

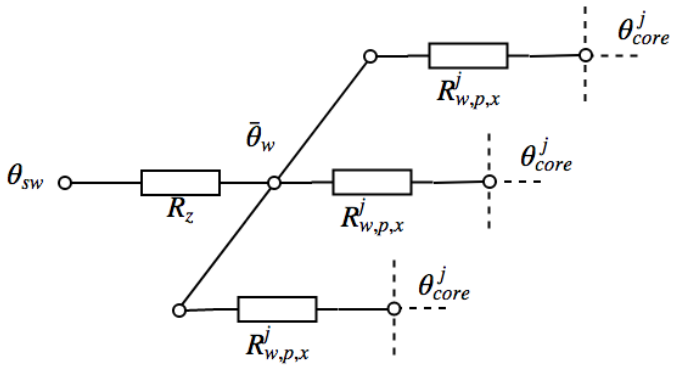

Figure 2.8: HiLo TABS RC part from supply water temperature to core temperature.

Additionally, it is now clear how all subsections start from the same mean water temperature. In order to direct the different heat fluxes into each subsection, area ratios before each resistance and capacitance term are used. Equation 2.2 shows resistance in z-direction with the added area ratio.

$$R_z = \frac{A_{fl}}{\sum_{j=1}^{N} A^j_{ta}} \frac{1}{2\,\dot{m}_{sp}\,c_w} \tag{2.2}$$

The ratio takes total TABS floor area A_{fl} over the area where the resistance or capacitance value sits in. In Equation 2.2, this area is all N activated TABS areas summed up. Different area ratios are used for different R and C values throughout the model, in order to sent the correct amount of thermal energy through the corresponding part of the TABS model, better shown in Section 2.2.5 with a full model overview. Water specific heat capacity is c_w and $\dot{m}_{sp}$ represents specific mass flow, as seen in Equation 2.3, where $\dot{m}$ is water mass flow, d_x is pipe spacing and l is pipe length.

$$\dot{m}_{sp} = \frac{\dot{m}}{d_x\,l} \tag{2.3}$$

On the other hand, the different $R^j_{w,p,x}$ use only their specific activated TABS area and not the summation of them, as shown in (2.4) - (2.6).

$$R^j_w = \frac{A_{fl}}{A^j_{ta}} \frac{d_x}{\pi\,\lambda_w} \left(49.03 + 4.17\,\frac{4\,\dot{m}^j_{sp}\,c_w\,d_x}{\lambda_w\,\pi}\right)^{-\frac{1}{3}} \tag{2.4}$$

$$R^j_p = \frac{A_{fl}}{A^j_{ta}} \frac{d_x \ln\left(\dfrac{\delta}{\delta - 2\,d_p}\right)}{2\,\pi\,\lambda_p} \tag{2.5}$$

$$R_x^j = \frac{A_{fl}}{A_{ta}^j} \frac{d_x \frac{1}{3} \left(\frac{d_x}{\pi \delta} \right)}{2 \pi \lambda_s} \tag{2.6}$$

Water thermal conductivity is defined as λ_w, supporting layer (where the pipe is embedded) thermal conductivity is λ_s, pipe outside diameter is δ and pipe thickness is d_p. Furthermore, specific water mass flow changes as pipe length changes from length per loop in R_z to length per subsection in R_w^j, represented in Equation 2.7.

$$\dot{m}_{sp}^j = \frac{\dot{m}}{d_x \, l^j} \tag{2.7}$$

Finally, mean water temperature $\bar{\theta}_w$, in case of N subsections, is calculated with Equation 2.8.

$$\bar{\theta}_w = \frac{\frac{\theta_{sw}}{R_z} + \sum_{j=1}^{N} \frac{\theta_{core}^j}{R_{w,p,x}^j}}{\frac{1}{R_z} + \sum_{j=1}^{N} \frac{1}{R_{w,p,x}^j}} \tag{2.8}$$

2.2.3 Core Temperature

Figure 2.9 shows the RC model part of standard TABS. Such a configuration can be used for HiLo's floor TABS, as they are fully encaptured by the building envelope.

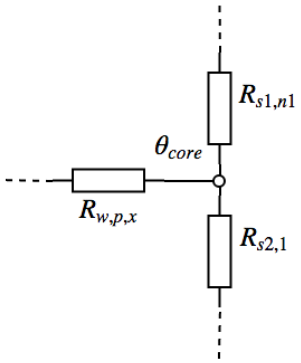

Figure 2.9: Standard TABS RC part of core temperature node.

Roof TABS in HiLo differ in a way, that they are an external surface, where its sides are exposed to ambient. Therefore, a linear edge loss is added, connecting core

temperature to outside air temperature θ_{oa} over an edge loss resistance value R_{el}, shown in Figure 2.10.

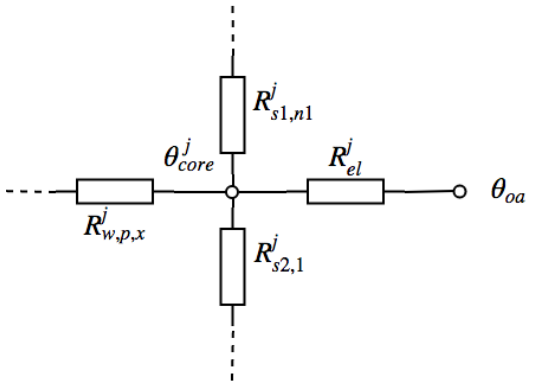

Figure 2.10: Roof TABS RC part of core temperature node with the added connection to outside air over edge loss resistance.

Nodal temperature calculation for the standard models core, in case of floor TABS, is given with

$$\theta_{core} = \frac{\frac{\bar{\theta}_w}{R_{w,p,x}} + \frac{\theta_{s1,n1}}{R_{s1,n1}} + \frac{\theta_{s2,1}}{R_{s2,1}}}{\frac{1}{R_{w,p,x}} + \frac{1}{R_{s1,n1}} + \frac{1}{R_{s2,1}}} \tag{2.9}$$

whereas the calculation for the roof TABS changes to

$$\theta^j_{core} = \frac{\frac{\bar{\theta}_w}{R^j_{w,p,x}} + \frac{\theta^j_{s1,n1}}{R^j_{s1,n1}} + \frac{\theta^j_{s2,1}}{R^j_{s2,1}} + \frac{\theta_{oa}}{R^j_{el}}}{\frac{1}{R^j_{w,p,x}} + \frac{1}{R^j_{s1,n1}} + \frac{1}{R^j_{s2,1}} + \frac{1}{R^j_{el}}} \tag{2.10}$$

The added edge loss resistance is visible at the end of Equation 2.11 by the two terms including R_{el} and defined by (2.11). Numerator λ^j_{el} depicts linear edge loss in $\frac{W}{m\,K}$ and denominator l^j_e is the length of the edge exposed to ambient in m.

$$R^j_{el} = \frac{\lambda^j_{el}}{l^j_e} \tag{2.11}$$

From core temperature the model expands vertically in both positive and negative y-direction through the different layers, which are modelled through a resistance and a capacitance, shown in Figure 2.2 in Section 2.2. The vertical branch in parallel represents

the floor area, where no pipes are embedded. Thus, it model a normal floor with no heating or cooling capability, called from now on unactivated area. Such an area is observable, for example, on the edges of subsection 1 in Figure 2.5, Section 2.2.1. For the activated part, general vertical layer resistance and capacitance values are calculated by (2.12) and (2.13). Note the area ratio of C is just the reciprocate of the one of R.

$$R_s^{j,k} = \frac{A_{fl}}{A_{ta}^j} \frac{d_{s,y}^k}{\lambda_s^k} \tag{2.12}$$

$$C_s^{j,k} = \frac{A_{ta}^j}{A_{fl}} d_{s,y}^k \rho_s^k c_s^k \tag{2.13}$$

As superscript j differentiates between subsections in the x-z plane, k depicts each layer's position in y-direction. For one such layer it is possible to change its $d_{s,y}^k$ per subsection to account for the varying thickness in HiLo's TABS. Resistance and capacitance calculations then change to Equations 2.14 and 2.15, where $d_{s,y}^k$ becomes $d_{s,y}^{j,k}$.

$$R_s^{j,k} = \frac{A_{fl}}{A_{ta}^j} \frac{d_{s,y}^{j,k}}{\lambda_s^k} \tag{2.14}$$

$$C_s^{j,k} = \frac{A_{ta}^j}{A_{fl}} d_{s,y}^{j,k} \rho_s^k c_s^k \tag{2.15}$$

Indices s and u are used to differentiate between activated (slab) and unactivated area, where the calculation of R_u and C_u is the same as for R_s and C_s, except for the area ratio, shown in (2.16) and (2.17).

$$R_u^{j,k} = \left(\frac{A_{fl}}{A_{fl}^j - A_{ta}^j} \right) \frac{d_{u,y}^k}{\lambda_u^k} \tag{2.16}$$

$$C_u^{j,k} = \left(\frac{A_{fl}^j - A_{ta}^j}{A_{fl}} \right) d_{u,y}^k \rho_u^k c_u^k \tag{2.17}$$

Additionally, varying layer thickness R and C values use the same principle that is used for the activated area, shown in Equations 2.18 and 2.19.

$$R_u^{j,k} = \left(\frac{A_{fl}}{A_{fl}^j - A_{ta}^j} \right) \frac{d_{u,y}^{j,k}}{\lambda_u^k} \tag{2.18}$$

$$C_u^{j,k} = \left(\frac{A_{fl}^j - A_{ta}^j}{A_{fl}} \right) d_{u,y}^{j,k} \rho_u^k c_u^k \tag{2.19}$$

2.2.4 Surface Temperature

As already mentioned in Section 2.2, the TABS model for HiLo only spans from supply water temperature to surface temperatures. At the surface, the individual subsections in parallel join back together, as shown in Figure 2.11. Therefore, the assumption that a surface layer has uniform temperature and a uniform capacitance value is made.

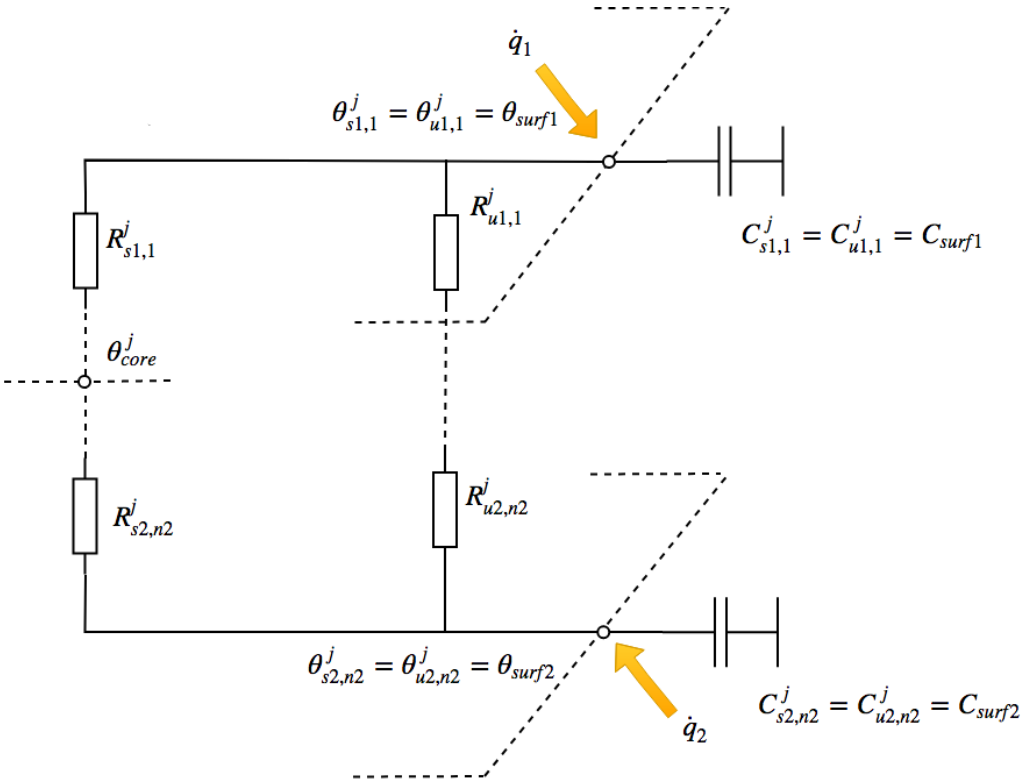

Figure 2.11: HiLo TABS uniform surface layer temperature interface with TRNSYS. MATLAB receives heat fluxes $\dot{q}_1$ and $\dot{q}_2$ from room to surfaces and sends surface temperatures θ_{surf1} and θ_{surf2} back to TRNSYS.

Here is where the interface between MATLAB and TRNSYS is. Outputs from TRNSYS to MATLAB are heat fluxes $\dot{q}_1$ and $\dot{q}_2$ from room to surface layers, and outputs from MATLAB to TRNSYS are surface temperatures θ_{surf1} and θ_{surf2}, as shown with Figure 2.11. The area ratio for the uniform capacitance value becomes 1, presented by (2.20).

$$C = \frac{\sum_{j=1}^{N} A^j_{fl}}{A_{fl}} \; ... = 1 \; ... \tag{2.20}$$

Surface layer temperatures are then calculated with (2.21) and (2.22).

$$\frac{d\theta_{surf1}}{dt} = \frac{1}{C_{surf1}} \left(\sum_{j=1}^{N} \left(\frac{\theta^j_{s1,1} - \theta_{surf1}}{R^j_{s1,1}} + \frac{\theta^j_{u1,1} - \theta_{surf1}}{R^j_{u1,1}} \right) + \dot{q}_1 \right) \tag{2.21}$$

$$\frac{d\theta_{surf2}}{dt} = \frac{1}{C_{surf2}} \left(\sum_{j=1}^{N} \left(\frac{\theta^j_{s2,n2} - \theta_{surf2}}{R^j_{s2,n2}} + \frac{\theta^j_{u2,n2} - \theta_{surf2}}{R^j_{u2,n2}} \right) + \dot{q}_2 \right) \tag{2.22}$$

2.2.5 Full Model Overview

A simplified full model overview with three subsections is shown in Figure 2.12. Non surface capacitances and some vertical layer resistances are not drawn to keep the figure clear. The focus lays on the different area ratios, which are depicted with different colors for each part of the TABS model.

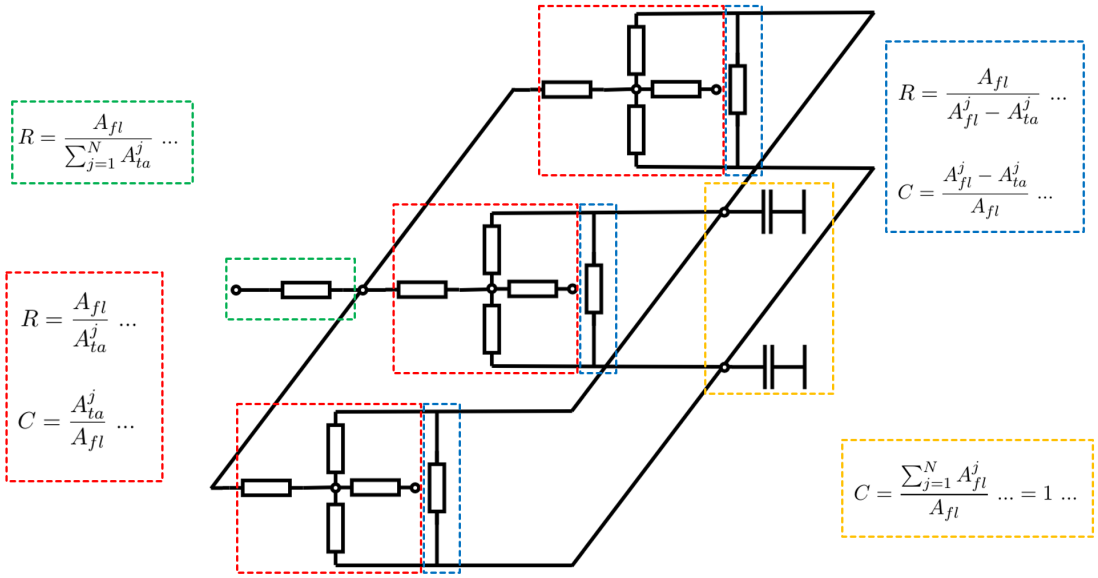

Figure 2.12: Full model overview of HiLo TABS RC model (without non surface resistance and capacitance parts for clarity) with three subsections. Different areas are highlighted in different colors with their corresponding TABS area ratios.

A more detailed full model overview with three subsections and arbitrary vertical layer configuration is presented in Figure 2.13.

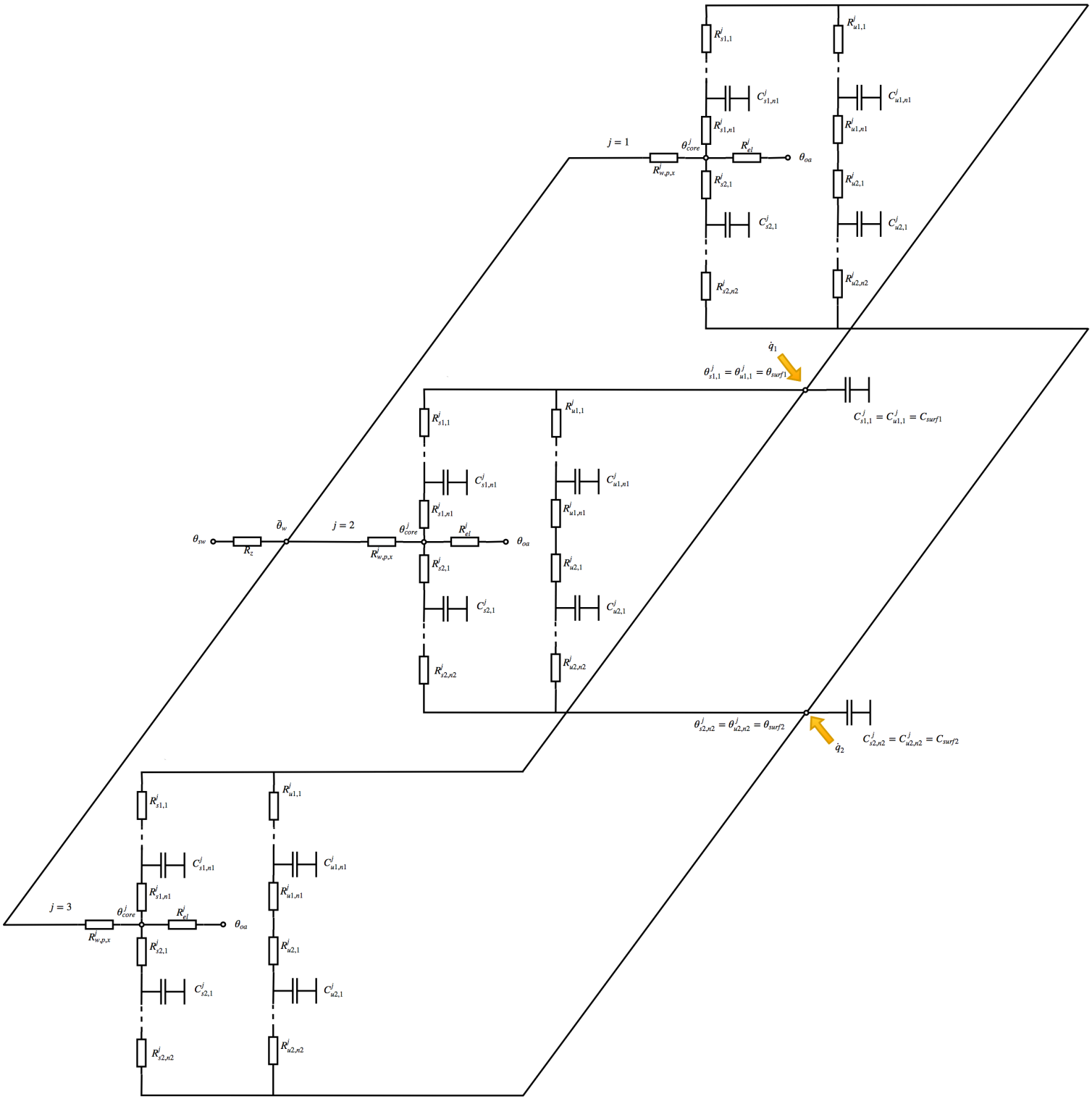

Figure 2.13: Full model overview of HiLo TABS RC model with three subsections and arbitrary vertical layer configuration.

2.3 TRNSYS TABS Model Implementation

2.3.1 Floor TABS

A first idea to implement the floor TABS model into TRNSYS was through defining two massless, highly resistive layers and fitting the MATLAB model in between them, as shown in Figure 2.14 on the left.

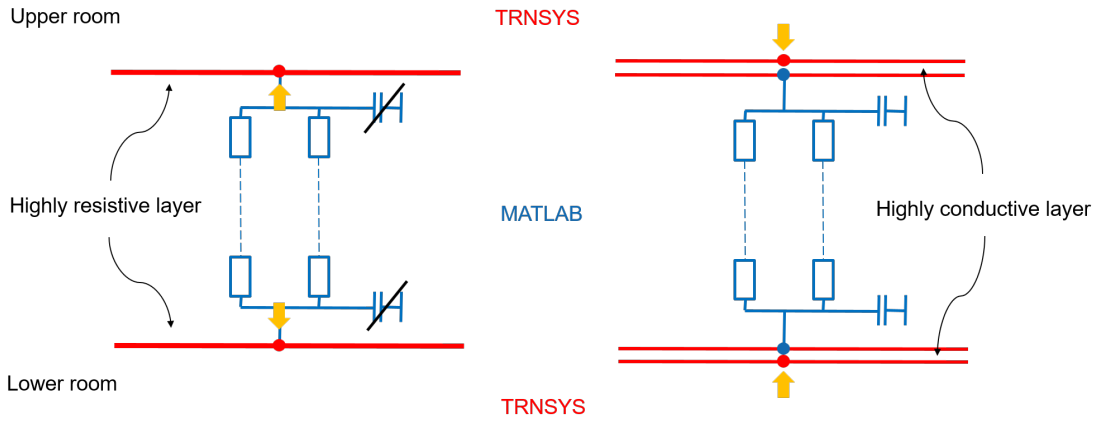

Figure 2.14: Implementation of floor TABS into TRNSYS. On the left is a first approach where TRNSYS receives an inside heat flux to surface and sends back a surface temperature. On the right is a second approach where TRNSYS receives a surface temperature and sends back a heat flux from room to inside surface.

One layer represents the floor surface in the upper room and the other the ceiling of the lower room. MATLAB receives surface temperatures, calculated by TRNSYS, and outputs two heat fluxes to the inside surfaces of TRNSYS' floor and ceiling layers. The problem with this approach is, that the capacitances of both surface layers are neglected. For them to be included, the massless, highly resistive layers in TRNSYS would have to be changed to massive layers, where the capacitances of the surface layers are included. However, the TABS model is then split, as surface layers are defined in TRNSYS and the rest in MATLAB, which is not a clean method. Additionally, if layer configuration would have to be changed, it would have to be done twice. First, in MATLAB's EXCEL input file and second in TRNSYS' Type 56 building component TRNBuild.

Another approach was chosen, where MATLAB includes the calculation of surface temperatures. TRNSYS then receives surface temperatures and calculates heat fluxes to the inside surfaces through radiative and convective parts from the room. Capacitance values of the surface layers are now included in MATLAB's part and the interface between the two programs is cut at the surface of the TABS model.

To implement this approach into TRNSYS, the highly resistive layers are now replaced with highly conductive layers, which are defined in TRNBuild as boundary walls. On their backside, it is possible to define boundary temperatures, which take the calculated

surface temperatures from MATLAB as input values. Through the high conduction of the layers, the backside temperatures are now forced onto the inside surfaces of the layers.

2.3.2 Roof TABS

Implementation of the roof TABS into TRNSYS is a different story. The floor TABS sit in between two rooms, each being defined as a thermal zone in TRNSYS. The floor of the upper room and the ceiling of the lower room can be defined as boundary walls and each given an input temperature from MATLAB. At the roof on the other hand, there is a thermal zone below but the outside above, thus no thermal zone. Consequently, it is not possible to define another surface, which can receive the upper surface temperature calculated by MATLAB. TRNSYS would now take the lower surface temperature as outside surface temperature and use it for radiative and convective heat transfer calculations, which would not be correct. Therefore, the model is extended to span all the way to sky temperature θ_{sky} for radiative and to outside air temperature θ_{oa} for convective calculations, shown in Figure 2.15.

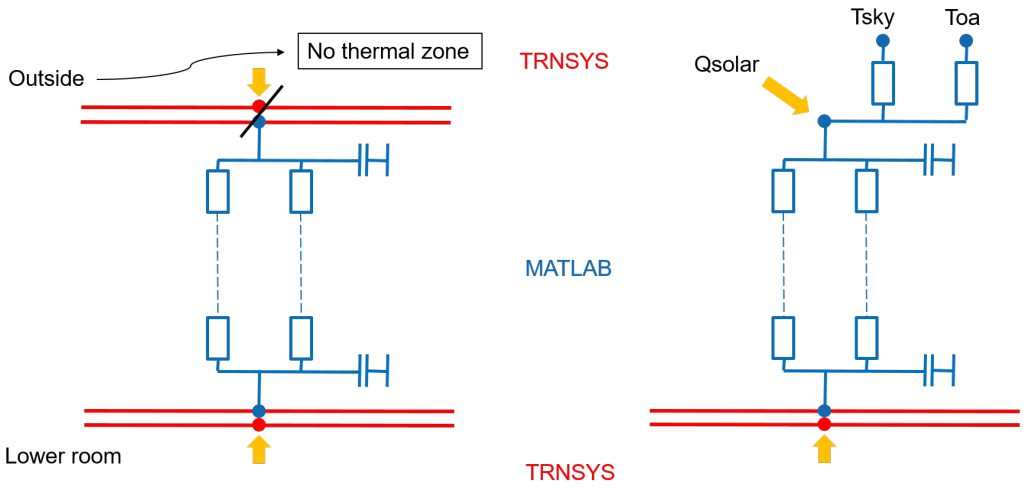

Figure 2.15: Implementation of roof TABS into TRNSYS. On the left is the concept for floor TABS, which is not applicable anymore. On the right is an adjusted concept for roof TABS, which extends to sky and outside air temperature to include radiative and convective heat fluxes, respectively. Additionally, TRNSYS sends solar heat gains on the roof surfaces to MATLAB.

MATLAB now receives a solar heat flux at the upper surface and a heat flux from the room at the lower surface. It calculates surface temperatures and sends the lower one back to TRNSYS. Top surface layer temperature calculation changes from

$$\frac{d\theta_{surf1}}{dt} = \frac{1}{C_{surf1}} \left(\sum_{j=1}^{N} \left(\frac{\theta^j_{s1,1} - \theta_{surf1}}{R^j_{s1,1}} + \frac{\theta^j_{u1,1} - \theta_{surf1}}{R^j_{u1,1}} \right) + \dot{q}_1 \right) \tag{2.23}$$

to

$$\frac{d\theta_{surf1}}{dt} = \frac{1}{C_{surf1}} \left(\sum_{j=1}^{N} \left(\frac{\theta^j_{s1,1} - \theta_{surf1}}{R^j_{s1,1}} + \frac{\theta^j_{u1,1} - \theta_{surf1}}{R^j_{u1,1}} \right) + \dot{q}_{solar} + \dot{q}_{rad} + \dot{q}_{conv} \right), \tag{2.24}$$

with

$$\dot{q}_{rad} = \sigma \epsilon (\theta^4_{sky} - \theta^4_{surf1}) \tag{2.25}$$

and

$$\dot{q}_{conv} = h(\theta_{oa} - \theta_{surf1}) \,. \tag{2.26}$$

2.4 Ventilation

CONTAM's sophisticated airflow calculations are used for modelling of HiLo's natural and mechanical ventilation systems. Figure 2.16 shows CONTAM's sketchpad of a simple example room, where different air flow components, which are used in this thesis, are defined.

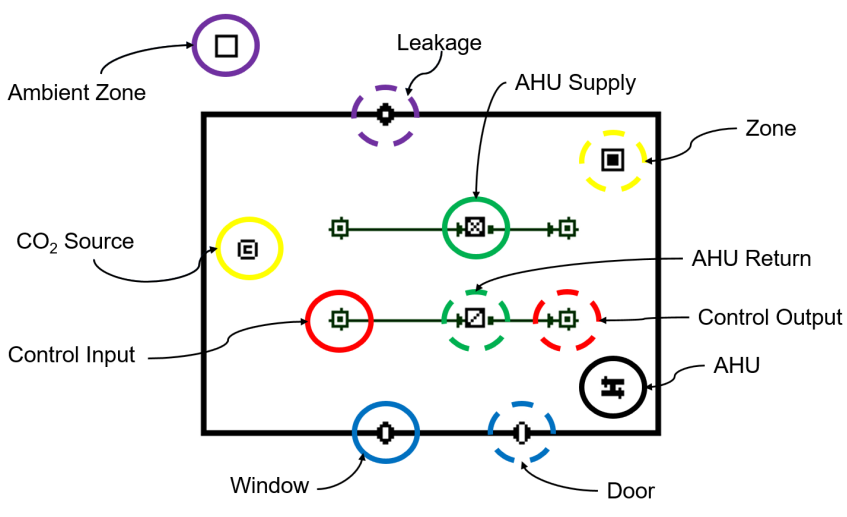

Figure 2.16: CONTAM's sketchpad with different airflow components used for the natural and mechanical ventilation model.

The black rectangular defines an air zone, which is equivalent to a thermal zone in TRNSYS. Parameters like zone volume, height, floor area can be set and the zone is defined through the icon marked in the yellow-dashed circle. An ambient zone needs to be defined outside of the building, marked here in violet. Air flow paths such as leakages, windows and doors can be defined between zones, encircled in violet-dashed, blue and blue-dashed, respectively. Air handling units can be created to account for mechanical ventilation, marked in black. Their supply and return points can be defined, which can be put in the same or another zone, here apparent in green and green-dashed, respectively. Furthermore, contaminant sources such as CO_2 can be defined to account for occupants in the building, marked in yellow. Finally, inputs and outputs between CONTAM and TRNSYS can be set for controls of windows, AHUs and CO_2 generation as well as measure air flows and CO_2 levels, encircled in red and red-dashed.

2.5 Elechtrochromic Glass

A large glass facade encaptures HiLo's south and west facing sides. Most window glazings on these sides are made with electrochromic glass of the specific type SageGlass®Climatop. It has four different tinting states, which are all imported as different glazings in TRNSYS' window library. After defining each window in TRNBuild, it is possible to define a specific glazing for each window by giving it the corresponding glazing ID, shown in Figure 2.17. This window ID can be set to constant or as an input to TRNBuild. To be able to switch between different glazing states, it is set as an input and sent from the electrochromic glass controller from MATLAB to TRNBuild.

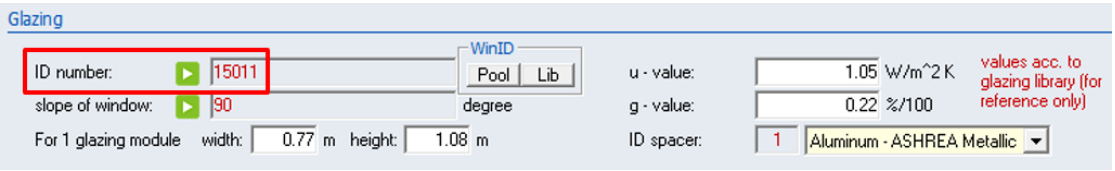

Figure 2.17: TRNBuild's way of changing window states through choosing glazing IDs, which can be set as constant or as input, e.g. from MATLAB.

When a window ID is set as an input, in the first timestep it seems to be 0, no matter the input number. This is assumed to happen because the input to TRNBuild is sent after initializing the 3D multizone building, even though MATLAB is set to be run before TRNBuild in the component order of TRNSYS. Therefore, a window ID of 0 is chosen for the clear state and 1, 2 and 3 are chosen for the two intermediate and dark state, respectively. Consequently, a simulation will always start with a clear window state in the first timestep.

2.6 3D Geometry

Modelling HiLo's 3D geometry is part of the coupling process of CONTAM and TRNSYS. A detailed description can be found in CONTAM's documentation [32]. It starts by creating a CONTAM project file, which is then exported to a TRNSYS 3D file (T3D) with help of the CONTAM 3D Exporter. It can then be imported into Google SketchUp, where its geometry can be adjusted. Figure 2.18 shows HiLo's T3D file opened in SketchUp.

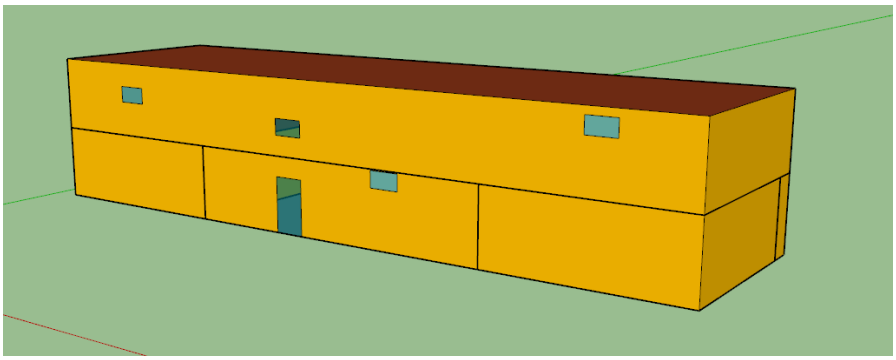

Figure 2.18: CONTAM's view of HiLo's 3D geometry opened in SketchUp. Only natural ventilation openings are visible, as they are the only thing necessary for CONTAM's air flow calculations.

What is shown here is actually what CONTAM sees for its airflow calculations. It only needs window openings, which are used for natural ventilation. HiLo's big glass facade is unimportant to CONTAM, as thermal calculations are all done in TRNSYS. At this step, the model can be checked for errors, which can sneak in when defining windows, which might fall outside of their wall surface. This can happen when one isn't careful when defining the windows position on the wall as well as its relative height to the level it is defined in.

Next, the model can be adjusted to better fit its 3D geometry. At this stage, it is only necessary to define the right amount of wall and window surfaces. HiLo's adjusted geometry is shown in Figure 2.19.

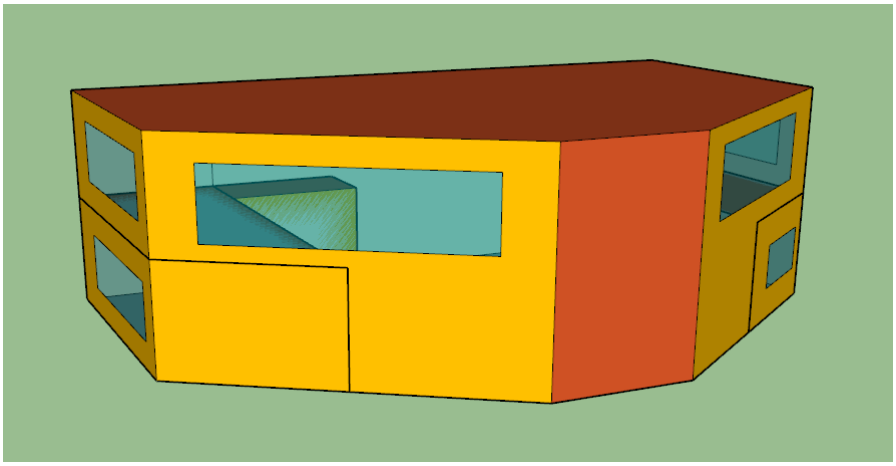

Figure 2.19: HiLo's modified 3D geometry for TRNBuilds thermal calculations opened in SketchUp. Natural ventilation openings are not modelled anymore, as they do not matter to TRNBuild and are already included in CONTAMs project file. Surface areas are not yet proportionate, as they will be changed in a later stage.

Natural ventilation openings are not necessary anymore, as they don't matter to TRNSYS, but only to CONTAM and are already defined in its project file. Proportions of window, wall and roof surfaces are not yet important, as they will be changed in a next step. The red vertical wall represents the vertical part of the roof, which curves down and touches the ground. Lastly, after finishing the coupling process, TRNBuild's building file .b17 can be opened and edited. An excerpt of such is shown in Figure 2.20.

```
*-------------------------------------------------------------------------------------------------------------
*  Z o n e  1_8  /  A i r n o d e  1_8
*-------------------------------------------------------------------------------------------------------------
ZONE 1_8
RADIATIONMODE
 BEAM=STANDARD : DIFFUSE=STANDARD : LONGWAVE=STANDARD : GEOMODE=3D_DATA : FSOLAIR=0
AIRNODE 1_8
WALL   =M11          : SURF= 20 : AREA=      6.65 : ADJACENT=1_5 : ADJ_SURF=6 : BACK
WALL   =M3           : SURF= 21 : AREA=       2.8 : EXTERNAL : ORI=S_35_90 : FSKY=0.5
WINDOW=WINDOW_04     : SURF= 38 : AREA=      26.1 : EXTERNAL : ORI=S_35_90 : FSKY=0.5
WALL   =M11          : SURF= 22 : AREA=       4.5 : ADJACENT=1_6 : ADJ_SURF=11 : BACK : COUPL=INPUT 1*MIX_1_6_1_8
WALL   =M4           : SURF= 23 : AREA=       8.6 : EXTERNAL : ORI=N_180_90 : FSKY=0.5
WINDOW=WINDOW_01     : SURF= 41 : AREA=      16.4 : EXTERNAL : ORI=N_180_90 : FSKY=0.5
WALL   =M7           : SURF= 24 : AREA=      40.3 : BOUNDARY=20
WALL   =EXT_WALL     : SURF= 25 : AREA=      0.01 : EXTERNAL : ORI=W_90_90 : FSKY=0.5
WINDOW=WINDOW_05     : SURF= 40 : AREA=     11.19 : EXTERNAL : ORI=W_90_90 : FSKY=0.5
WALL   =M11          : SURF= 26 : AREA=      10.5 : ADJACENT=1_5 : ADJ_SURF=3 : BACK : COUPL=INPUT 1*MIX_1_5_1_8
WALL   =M11          : SURF= 27 : AREA=       8.6 : ADJACENT=1_7 : ADJ_SURF=18 : BACK : COUPL=INPUT 1*MIX_1_7_1_8
WALL   =BOUND_COND   : SURF= 29 : AREA=      11.5 : BOUNDARY=INPUT 1*TABS_T_ROOF_VER
WALL   =M11          : SURF= 30 : AREA=       5.7 : ADJACENT=1_5 : ADJ_SURF=2 : BACK : COUPL=INPUT 1*MIX_1_5_1_8
WALL   =M6           : SURF= 31 : AREA=      15.6 : EXTERNAL : ORI=E_270_90 : FSKY=0.5
WINDOW=WINDOW_02     : SURF= 39 : AREA=       2.1 : EXTERNAL : ORI=E_270_90 : FSKY=0.5
WALL   =M2           : SURF= 32 : AREA=     38.65 : BOUNDARY=20
WALL   =M3           : SURF= 33 : AREA=       2.3 : EXTERNAL : ORI=S_325_90 : FSKY=0.5
WINDOW=WINDOW_03     : SURF= 37 : AREA=      21.5 : EXTERNAL : ORI=S_325_90 : FSKY=0.5
WALL   =BOUND_COND   : SURF= 51 : AREA=        24 : BOUNDARY=INPUT 1*TABS_T_MAIN1
WALL   =BOUND_COND   : SURF= 35 : AREA=      19.5 : BOUNDARY=INPUT 1*TABS_T_MAIN2
WALL   =BOUND_COND   : SURF= 36 : AREA=     103.5 : BOUNDARY=INPUT 1*TABS_T_ROOF_HOR
WALL   =M11          : SURF= 49 : AREA=         3 : ADJACENT=1_6 : ADJ_SURF=10 : BACK
WALL   =M11          : SURF= 50 : AREA=      11.3 : ADJACENT=1_9 : ADJ_SURF=45 : BACK : COUPL=INPUT 1*MIX_1_9_1_8
```

Figure 2.20: Excerpt of HiLo's .b17 building file used for TRNBuild's thermal calculations. Surface areas, orientations, types (adjacent, external, boundary) and interzonal air flows are adjusted here.

Here, surface areas of windows, walls and roofs and their orientations can be modified. Additionally, recoupling of interzonal flows can be done as they might be lost during editing the geometry in Google SketchUp. Furthermore, boundary walls can be defined, which receive surface temperatures from MATLAB's TABS model.

2.7 Internal Longwave Radiation Calculation

HiLo's horizontal roof part has nine TABS loops and its vertical part has one. In order to give each roof patch the calculated TABS loop temperature, each has to be defined as a surface on its own. Figure 2.21 shows SketchUp's 3D model of HiLo's roof with such an approach.

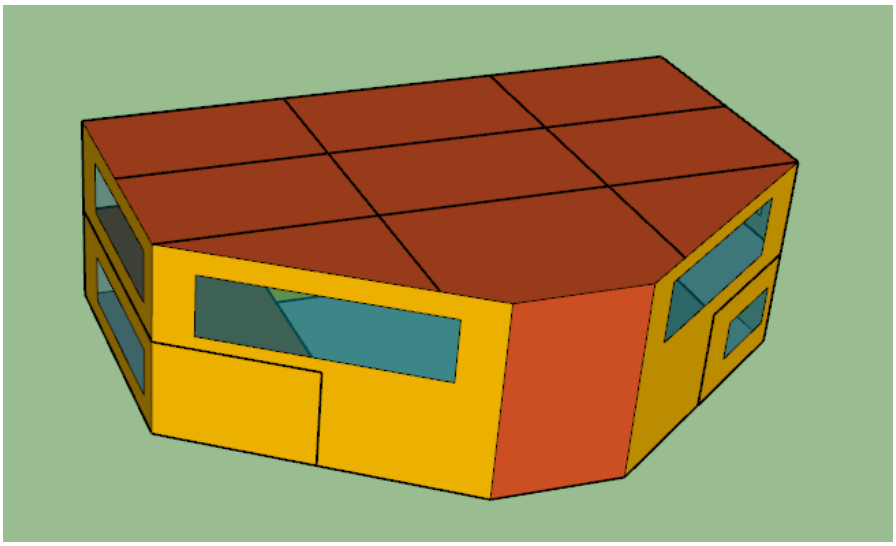

Figure 2.21: HiLo's roof with nine surface patches, each representing one TABS loop that receives its calculated surface temperature from the model in MATLAB. The red vertical surface is the vertical roof part, which curves down and touches the ground, and houses the tenth TABS loop.

TRNBuild offers a standard or detailed internal longwave radiation calculation mode. Here, the latter is not possible, because HiLo's geometry is not convex but concave, as shown in its simplified front view visualization in Figure 2.22

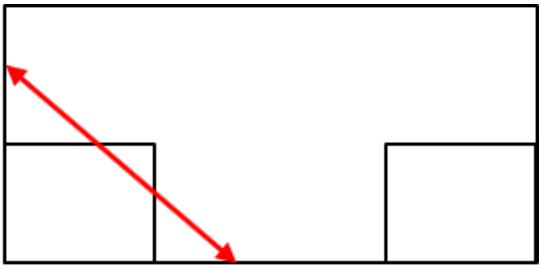

Figure 2.22: Simplified front view of HiLo's concave geometry, with which detailed longwave radiation calculation mode in TRNBuild cannot be applied.

Consequently, standard mode has to be chosen, which stands in conflict with the above presented approach of having one roof surface per TABS loop. Standard longwave radiation calculation uses a temperature starnode approach. It basically means, that each surface "sees" every other surface in the same thermal zone for its radiative heat exchange. It is assumed, that such an error would give erroneous heat flows between roof patches, as they are active TABS surfaces. Thus, a workaround had to be implemented as follows. Each roof patch TABS surface temperature is weighted averaged by its surface area over the whole horizontal roof surface. In SketchUp, one roof surface is created, which receives this averaged surface temperature, visible in Figure 2.23. By having one horizontal roof surface, no wrongful radiative calculations can be made between active surfaces.

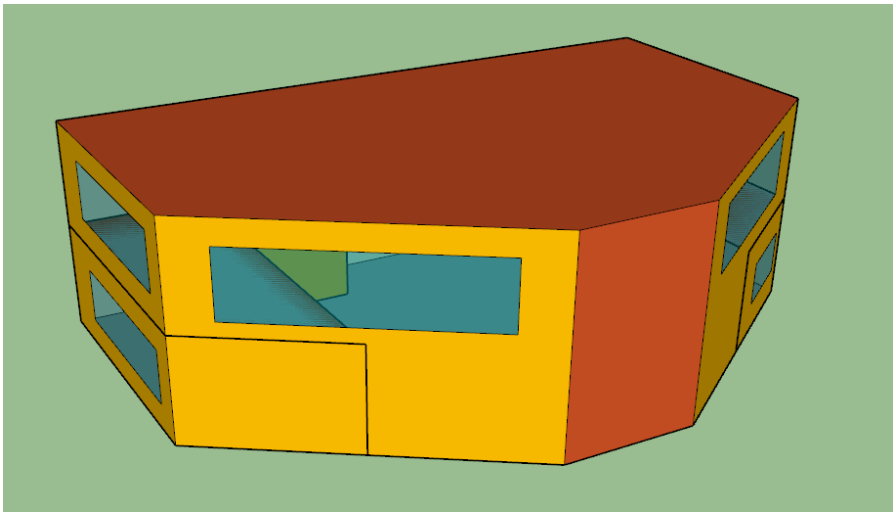

Figure 2.23: HiLo's horizontal roof as one surface, receiving an averaged TABS surface temperature from the model in MATLAB. The vertical part stays unchanged, as it only contains one loop.

The vertical roof part stays the same, as it only contains one TABS loop and therefore

only needs one surface. However, there is still an incorrect radiative heat flux calculation happening at HiLo's back side. As part of HiLo is against NEST, which is a heated zone, and another part of the same wall is against ambient, two surfaces have to be created, as shown in Figure 2.24.

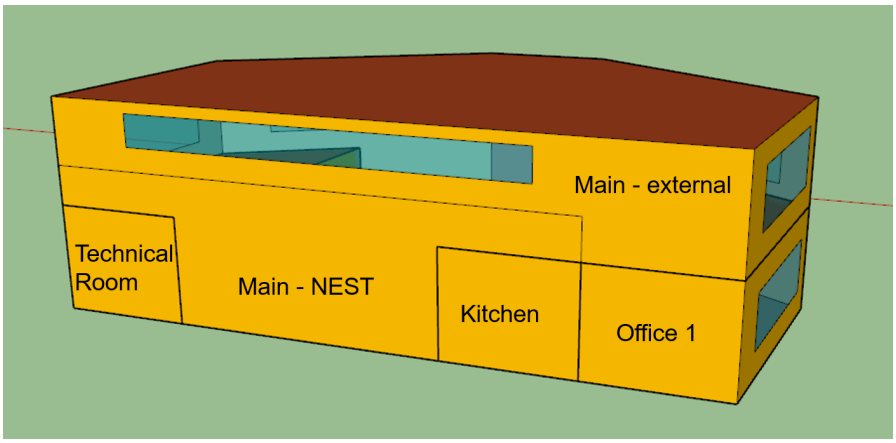

Figure 2.24: Backside of HiLo with Main Space surface split into the two patches Main - NEST and Main - external, which result in wrongful radiative calculations in the standard longwave radiation mode. Surfaces of Technical Room, Kitchen and Office 1 are not problematic, as they are in different thermal zones.

The surface against NEST receives a boundary temperature - same as TABS layers - of 22°C and the other is defined as external. These two surfaces "see" each other in standard longwave radiation calculation mode. However, since they are both passive surfaces where no TABS pipes are located near inside surfaces, as is the case with roof TABS, it is assumed that these incorrect calculations have a negligible effect on HiLo's whole building simulation.

2.8 Convective Heat Transfer Coefficient Calculation

Convective heat transfer coefficients (CHTC) for radiant heating and cooling systems depend on their surface slopes and their mode of operation, e.g. heating or cooling [33]. As HiLo's roof is quite curvy, surface angles are included in CHTC. Each subsection can be given a surface slope and since it is technically possible to define as many subsections as possible, the surface curvature can be captured to some extent. CHTC for ceilings, walls and floors are taken from [34] and linearly averaged for surface slopes in between. The calculated CHTC are sent from MATLAB to TRNSYS to be set as an input for active walls' inside surfaces.

Since the horizontal roof in SketchUp's T3D file is modelled as one surface, due to standard longwave radiation calculations explained in Section 2.7, TRNBuild can only receive one surface temperature. Therefore, the roof has to be approximated to work

with the condition of one roof surface set by the 3D model. Figure 2.25 shows the simplified approximation process of the horizontal roof part with its different resolution levels. Green is a high resolution level, where CHTC are calculated per TABS subsection. Blue represents a medium resolution level of CHTC per TABS loop and red shows a low resolution level of CHTC per whole horizontal roof surface.

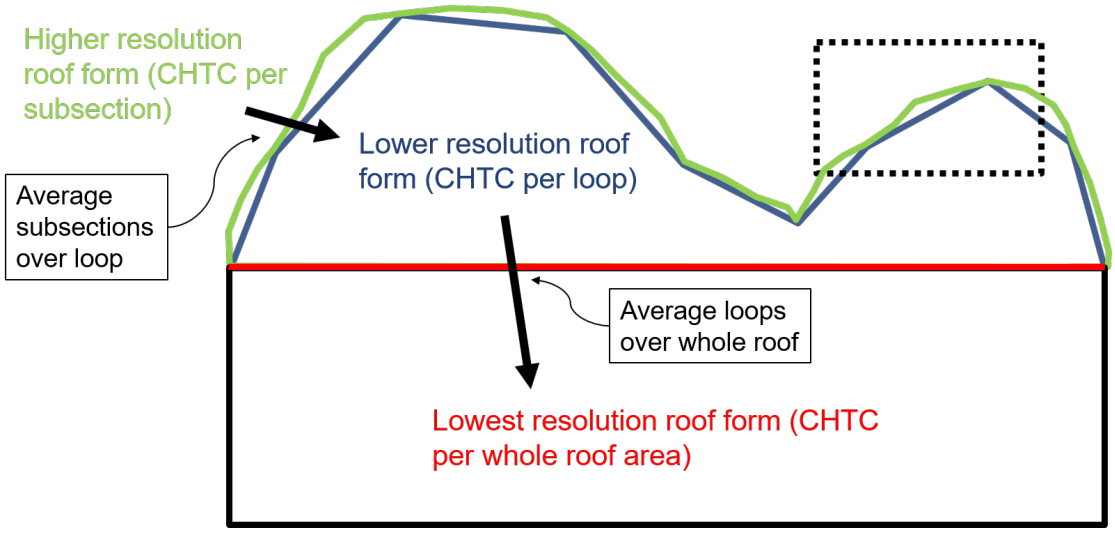

Figure 2.25: HiLo's roof and its different resolution levels for CHTC calculations. Green represents the calculation of CHTC per subsection (high resolution level) in MATLAB. Blue shows the averaged CHTC per loop (medium resolution level) and red is the further averaged CHTC per whole roof surface, which is then sent to TRNBuild.

A closer look at one of roof TABS loops is presented in Figure 2.26, marked as the black-dashed rectangular in Figure 2.25. It shows heat transfer of each subsection from the TABS model, simplified here for clarity, through its surface and over an inside convective heat transfer to room temperature. Each resistance represents the two bottom surface resistances in Figure 2.11, Section 2.2.4.

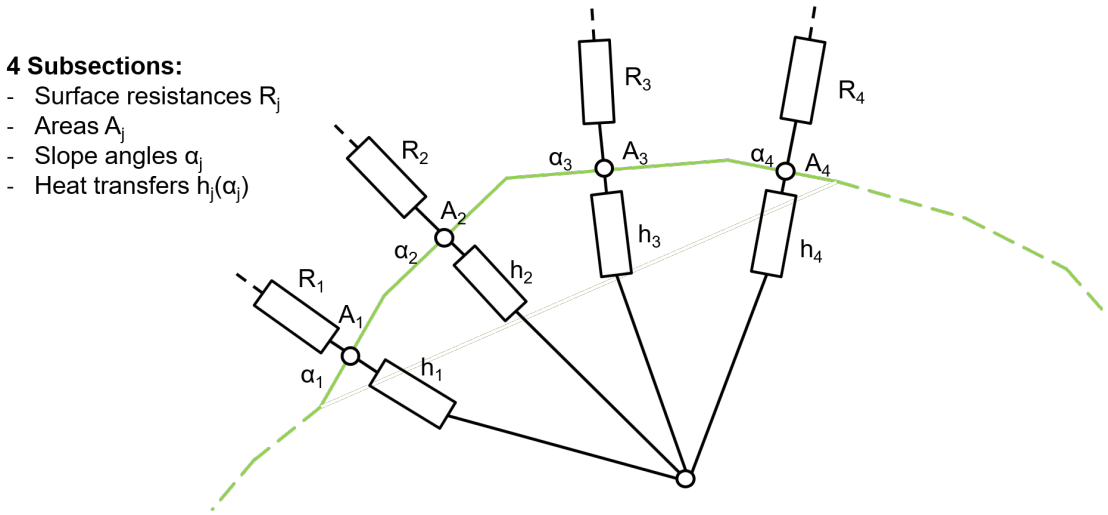

Figure 2.26: Magnified view of black-dashed sector marked in Figure 2.25, which shows a simplified visualization of one convective heat transfer, with its corresponding CHTC, from each subsection of roof TABS to room air. Both bottom surface resistance values from a subsection visible in Figure 2.11, Section 2.2.4 are represented by each of the resistances shown here.

Figure 2.27 presents the approximation step from resolution level high to medium, where CHTC are averaged per loop.

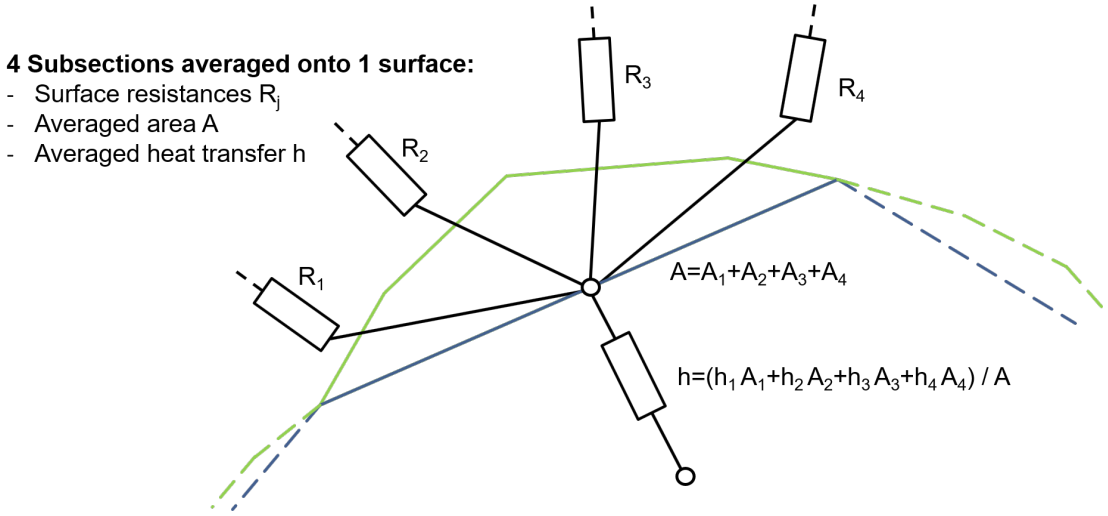

Figure 2.27: Magnified view of black-dashed sector marked in Figure 2.25, which shows a simplified visualization of one averaged convective heat transfer from an averaged surface temperature per loop to room air. Both bottom surface resistance values from a subsection visible in Figure 2.11, Section 2.2.4 are represented by each of the resistances shown here. CHTC are weighted averaged over their areas for each loop.

Furthermore, each CHTC per loop is then weighted averaged over the whole horizontal roof surface, which changes resolution level from medium to low. Finally, one total averaged inside CHTC is sent from MATLAB to TRNSYS where it is used for room side thermal calculations.

Outside CHTC depend on wind speed and are calculated through the correlation in Equation 2.27, with U_∞ being wind speed and h_e representing the external CHTC [35].

$$\begin{array}{ll} h_e = 4.0\,U_\infty + 5.6 & U_\infty < 5 \text{ m/s} \\ h_e = 7.1\,U_\infty^{0.78} & U_\infty > 5 \text{ m/s} \end{array} \tag{2.27}$$

Results and Discussion

In this chapter, each part of the full building model is presented and first simulation results are discussed to demonstrate their interaction witch each other.

3.1 MATLAB Code Structure

This thesis comes with five different MATLAB .m script files. One is a standalone, layer-wise fully adjustable TABS model made for comparison with a computational fluid dynamics (CFD) model (TABS_standalone_cfd_comparison.m). The other four files are only executable when being called by TRNSYS. The first one includes a TABS roof and floor model as well as ventilation, electrochromic glass and basic occupancy schedule input sections (hilo_control_1_vert_precise_hor_precise_2min.m). Both TABS models use detailed layer configuration and are fully adjustable. However, it is only possible to be run with a timestep of maximum two minutes. The next file is a copy of the second, with the difference being that it uses an averaging process by merging vertical TABS layers (hilo_control_1_vert_avg_hor_precise_30min.m). Hence, its layer configuration is not adjustable, as it is hard-coded which layers are merged together into which specific position. However, it can be run with a timestep of 30 minutes. These two files are being compared in a transient building simulation for justification of the vertical simplification process. The vertically averaged file is used as a base for the last two files. The first (hilo_control_2_vert_avg_hor_precise_30min.m) is model-wise the same as the base, but includes comments highlighting the differences between the comparison of itself to the last file (hilo_control_2_vert_avg_hor_avg_30min.m), which uses an averaging process of horizontal layer resolution. To summarize, files with names "hilo_control_1_*.m" and "hilo_control_2_*.m" are being compared for vertical and horizontal layer resolution simplification, respectively. For easy comparison of all files, it is advised to use MATLABs own "Compare" function.

It has to be noted, that no control part is implemented as of yet. Inputs to states are set in the Excel file and are kept for the whole simulation. For first transient test simulations, a simple controller is implemented, that sets states of natural and mechanical ventilation as well as active TABS to on or off at a predefined time. The code structure

of the averaged MATLAB - TRNSYS file, which includes all aspects of the other files, is laid out as follows.

1. Processing inputs and global parameters
   - Read in Excel input file (HiLo_model_specs_inputs.xlsx)
     - Parameters and states for all systems are saved here
   - Defining global parameters for all systems
   - Floor and roof TABS:
     - Calculate resistance and capacitance values
     - Averaging layers
     - Convective heat transfer coefficient (CHTC) calculations
   - Ventilation:
     - Natural ventilation states
     - Mechanical ventilation states
   - Electrochromic glass:
     - Window glazing ID (tinting state)
   - Occupancy schedule (occupancy is set to Mo-Fr 08:00-12:00, 13:00-17:00):
     - Number of people in each room
     - Number of PCs in each room
2. First timestep
   - Defining initial values
3. Each timestep
   - Basic control switches:
     - State of TABS, mechanical and natural ventilation
     - Change state of the above at a specific time in simulation (e.g. night cooling test case: turn system on after 72 hours, see Section 3.7)
   - Floor TABS:
     - Choosing right CHTC depending on heating or cooling case
     - Summing up rejoining heat fluxes from all subsections to surface layer
     - Calculating mean and return water temperatures
     - Calculating surface temperatures
     - Calculating layer temperatures of activated TABS area
     - Calculating layer temperatures of unactivated TABS area
   - Roof TABS (same as floor TABS with following addition):

  - Averaging CHTC per loop and further per whole horizontal roof surface
- Ventilation:
  - Defining latent and sensible efficiency of heat recovery and general air flows depending on mechanical ventilation states
  - Adding research AHU flows to return and supply points from AHU 1 and 2 in HiLo's main space
  - Office AHU flows for heat recovery are averaged, as return flows are from two different thermal zones with different properties
  - Atmosphere and pascal unit conversions for TRNSYS and CONTAM
- Electrochromic glass:
  - Relaying window glazing ID
- Occupancy schedule:
  - CO_2 gains per zone
  - Heat gains per zone

3.2 TRNSYS Deck File

When doing CONTAM - TRNSYS project coupling, a standard deck file is automatically created, which is shown in Figure 3.1. It is similar to a deck file created by the TRNSYS wizard for a 3D multizone building, with the addition of CONTAM's Type 98 and an atmosphere to pascal conversion component.

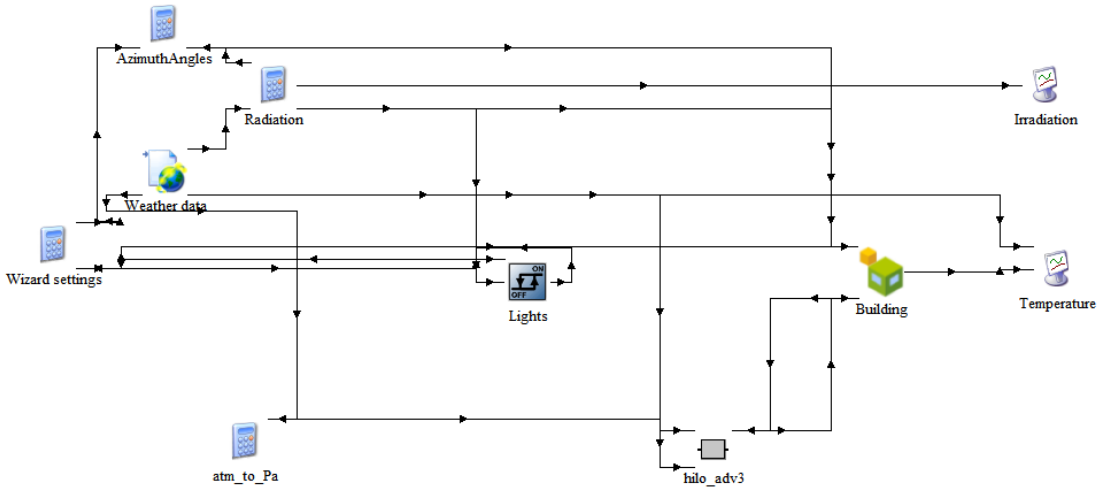

Figure 3.1: TRNSYS deck file automatically generated by the TRNSYS - CONTAM coupling process with its default components their connections to one another.

For HiLo's TRNSYS model, the following adjustments in the deck file are made.

1. Adding MATLAB's Type 155 component with the correct .m file path
2. Adding four different Type 667 heat recovery components
3. Moving atmosphere to pascal conversions into the MATLAB file
4. Adding six Type 65d online plotters for various data outputs of each system
5. Adding a Type 25c printer that writes various outputs to a file
6. Using the TURN function in the "Wizard settings" component to adjust rotation angle used for adapting azimuth angles

Figure 3.2 shows TRNSYS' modified deck file with each component and its connections.

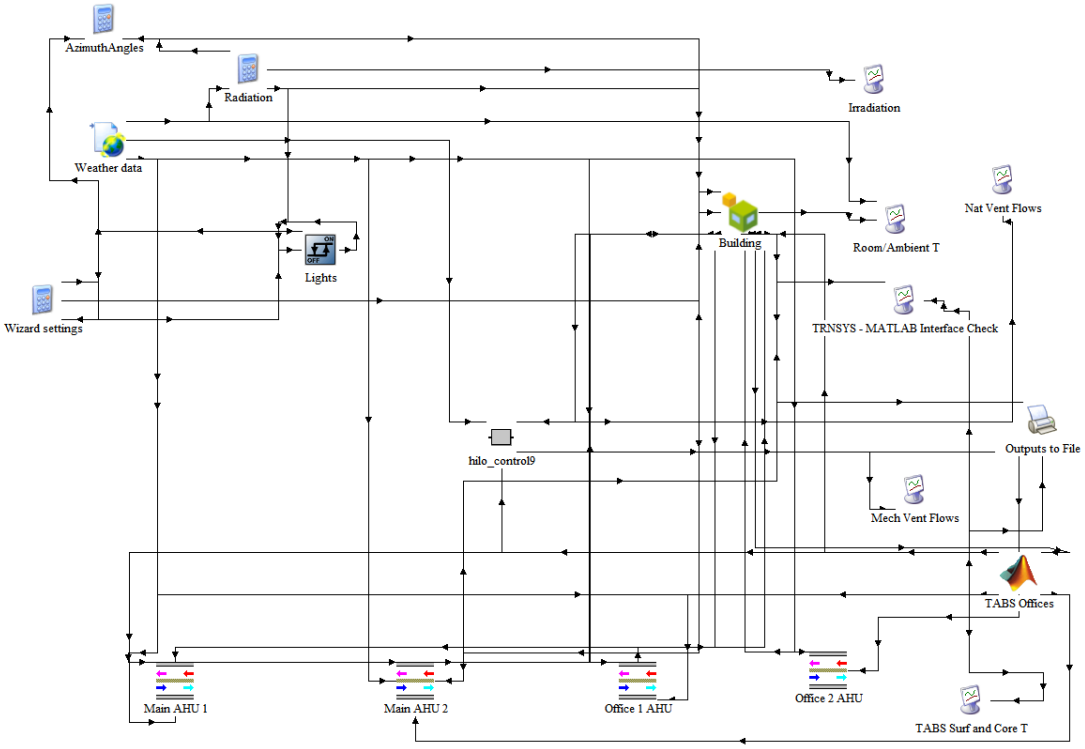

Figure 3.2: Full TRNSYS deck file for HiLo model with its components and their connections to one another.

Some outputs of MATLAB's Type 155 are left empty, as they were deleted during creation of MATLAB code and TRNSYS deck file. These can be used if additional outputs are needed. Otherwise, the number of outputs can always be redefined in its component parameters. To better view connections between components, one can use

"Table" view instead of "Classic" in the connection window.

What is still missing is an individual heat recovery unit for the research AHU. As its mass flow uses the same supply and return points as AHU 1 and 2 in HiLo's main space and the fact that it is not possible to define a return or supply point to two different AHU's in CONTAM, it is technically non-existent in CONTAM. As will be explained in more detail in Section 3.3, the additional mass flow is added to AHU 1 and 2 in MATLAB and sent to CONTAM via TRNSYS. With such an approach, it is impossible to model an additional heat recovery for the research AHU. TRNBuild receives one total air flow with one specific temperature per AHU defined in CONTAM. Since the research AHU is not modelled in CONTAM, its heat recovery does not have an individual input mass flow with corresponding temperature into TRNBuild. To include this, the CONTAM model would have to be changed to have three AHU's in Main Space and recoupled with TRNSYS.

Additionally, no pressure drops in heat recovery components are accounted for. As they depend on ducting system configuration, which is not defined at this stage, they cannot be estimated and will have to be set in the future.

3.3 CONTAM Model

The different air flow components discussed in Section 2.4 are here used to define HiLo's CONTAM model. Figure 3.3 shows the first floor with its room layout. Left and right are Office 1 and Office 2, respectively, and the large area in the middle is named Main Space. The small room at the top right is where electronic equipment is stored and called Technical Room. Inside Main Space on its top left is the Kitchen area.

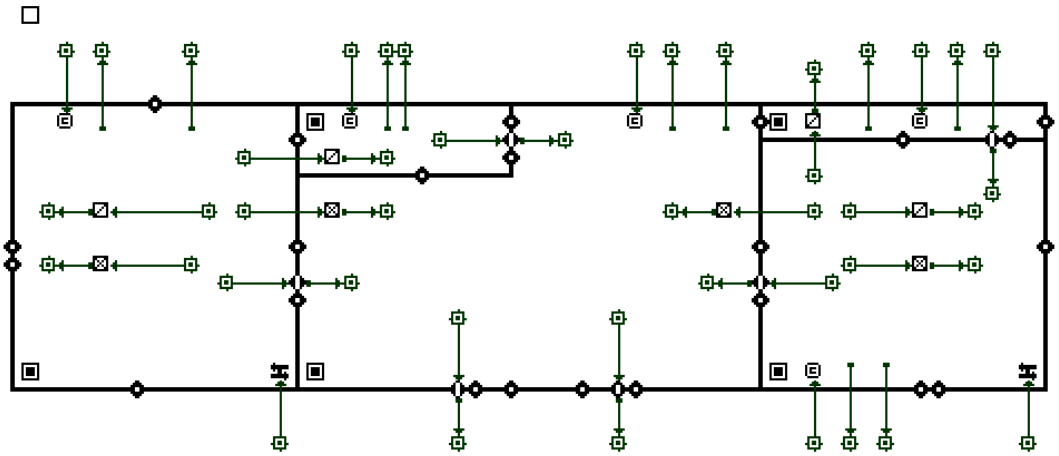

Figure 3.3: CONTAM model of HiLo's first level with its air flow components and their controls.

The two AHUs in the offices have each one supply and return point in their zones.

Additionally, Office 1 also has a supply point in Main space and a return point in Kitchen, whereas Office 2 has a supply point in Main Space, too, and a return point in Technical Room. Air flows of these return and supply points are individually controllable, as they are not in the same zone. CO_2 sources and sensors are in each zone. All components, except leakages, are fully controllable through inputs from MATLAB via TRNSYS.

Figure 3.4 shows HiLo's second floor, where two AHUs with each two supply and return points sit. Each supply and return mass flow is evenly divided by their supply and return points, as they are in the same zone, compared to the office return and supply points. Further, HiLo's research AHU is evenly coupled to each of the return/supply points of both AHUs for additional power. Hence, one forth of its return/supply mass flow is going to each return/supply point.

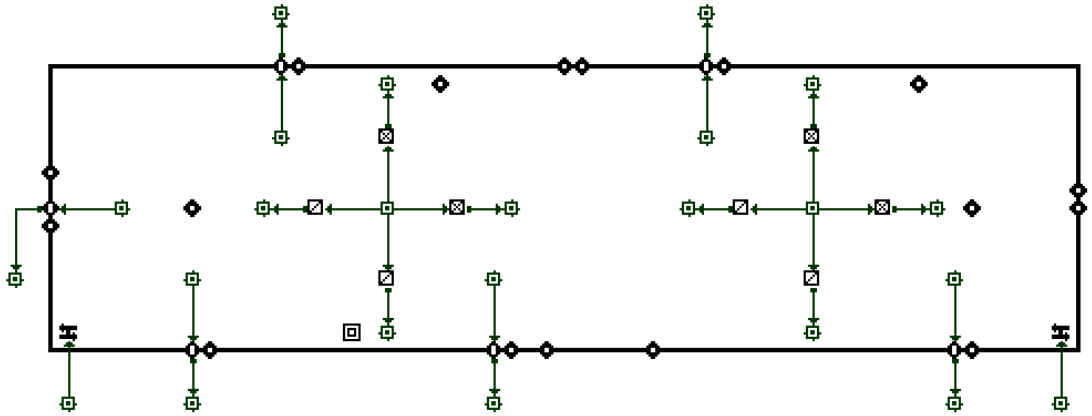

Figure 3.4: CONTAM model of HiLo's second level with its air flow components and their controls.

Leakages not placed on a wall account for vertical flows through ceilings and floors. One last roof leakage is visible in Figure 3.5. Leakage values of walls and windows are in flows per area, taken from ASHRAE library data [36] and multiplied by their area, whereas door leakages are defined per piece.

Figure 3.5: CONTAM model of HiLo's third level (roof outside surface) with its roof leakage.

Openings to ambient, e.g. windows and terrace door, use variable wind pressure data. Orientation, height, a wind pressure coefficient depending on surrounding terrain and a wind pressure profile taken from ASHRAE's library are defined to account for natural ventilation with necessary wind speed and direction being supplied by TRNSYS' weather file. A detailed mathematical description of these and all other air flow components can be found in CONTAM's documentation [32].

3.4 TRNSYS Internal Humidity Calculations Limitation

HiLo's Kitchen and Technical Room both have small zone volumes. These two rooms have each one AHU return point, as shown in Figure 3.3, Section 3.3. When mechanical ventilation is turned on and air is sucked out of these rooms, it has to be replaced by air coming in through leakages or doors from connected adjacent zones. Therefore, the flow of the return point strongly governs the rooms interzonal flows. When these are large, TRNSYS internal humidity calculations run into an error:

"Small internal timesteps (<0.1% of simulation timestep) used for humidity calculations due to large coupling air flows between zones!"

Only one meaningful explanation to this was found in TRNSYS' mail archive from 2006 [37]. The source actually targets TRNFlow in combination with COMIS, TRNSYS' old in house air flow calculation model. Still, it is assumed this might be the same problem here, as the error message is the same and the description of the problem applies here, too. It is explained, that there is an "outer" timestep (TRNSYS timestep) and then there is a smaller, "inner" timestep, in this case for example for humidity calculations. The inner timestep is $\frac{1}{10}$ of the smallest room time constant, which is calculated by zone volume divided by the total volume flow in and out of this zone. Thus, when having small rooms with big interzonal flows, internal timestep becomes very small. This is exactly the case in Kitchen and Technical Room. By decreasing timestep, increasing zone volume or decreasing interzonal flows, the error disappears.

As of now, return points in both rooms are turned off and connecting doors to adjacent zones are closed in order to do first simulations. In a next step, fine tuning between timestep and interzonal flows has to be done to find a working compromise.

3.5 Simplification of Vertical Layer Resolution

HiLo's TABS were first modelled with a timestep of 1 minute to ensure precision for a later validation by comparing it to CFD. For whole building simulations, the timestep was increased to 30 minutes, where the TABS model became unstable as temperatures started diverging. Equation 3.1 shows dependency of layer change in temperature on timestep and capacitance.

$$d\theta = \frac{dt}{C} \ ... \tag{3.1}$$

By having a large timestep and a small capacitance, change in temperature becomes big, which results in the TABS model becoming unstable. HiLo's TABS have multiple small layers with small capacitances. So when timestep is increased, these capacitances have to be increased, too. This can be achieved by merging adjacent layers together into one averaged layer, as shown in Figure 3.6.

Figure 3.6: Vertical layer averaging and merging process for TABS to increase layer capacitances. The top four layers above pipe level are merged into two layers, in case of roof TABS.

For the roof, the four top layers above the pipe are merged into two (case shown in Figure 3.6), whereas for the floor TABS the three top layers above the pipe are merged into one layer. Floor and roof TABS detailed configuration can be taken from HiLo's input Excel file (HiLo_model_specs_inputs.xlsx).

By merging multiple layers together, resulting capacitance becomes larger and timestep can be increased, thus computation time is saved. Additionally, with less layers, dimensions of nodal temperature matrices are decreased, which effectively decreases complexity and further saves computation time. A 3 day simulation with detailed layer configuration and a 1 minute timestep takes roughly 10 hours, whereas the same simulation with an averaged model and a 30 minute timestep takes only 40 minutes. This is on an old student machine with an i7-3770 3.40 GHz (8 CPUs). An online benchmark comparison with the latest Intel®CPU shows an increase in multicore computation of 108%. Therefore, computation time on a newer CPU can be roughly halved, resulting in about 20 minutes for a 3 day simulation.

To investigate how much precision is lost when decreasing vertical layer resolution, comparisons are made by simulating the detailed and averaged model. For the following comparisons in this section, simulation time is 48 hours and transient behavior is included by having TABS turned on for the first 16 hours, off for the next 16 and on again for the last 16 hours. Figure 3.7 shows TABS surface temperature differences between an averaged model with a 30 min timestep and a precise model with a 1 min timestep, called Simulation Case 1. The first term TABS 1 (TABS 2) stands for the TABS system above Office 1 (Office 2). The second term, Main or Office, stands for the room its corresponding surface is facing.

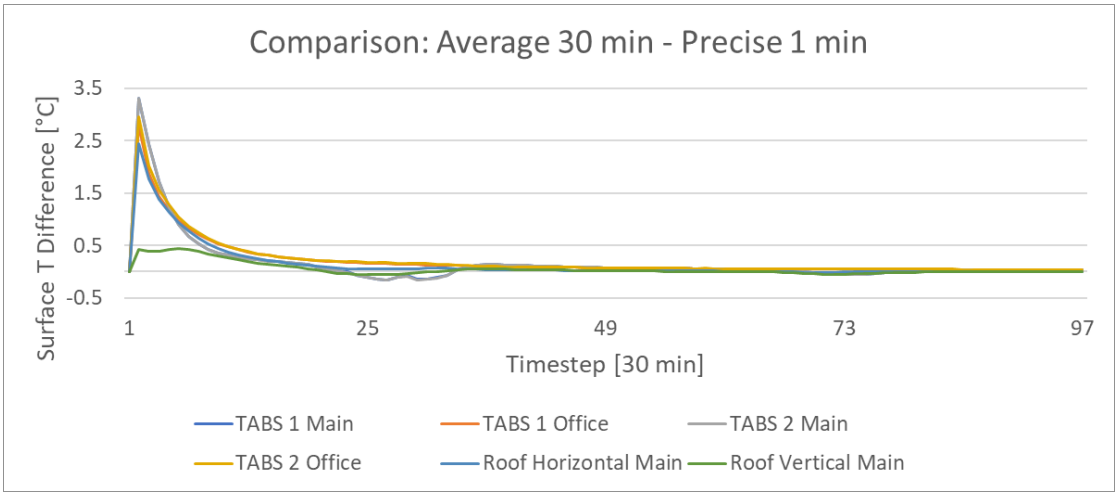

Figure 3.7: TABS surface temperature differences between the vertically averaged model with a 30 min timestep and the precise model with a 1 min timestep.

A big spike is visible in the beginning, which is assumed due to initializing of the individual nodal temperatures of the TABS model. At timestep 32 (16 hours) and 64 (32 hours), where transient switching of the TABS is happening, no big differences relative to before and after are observable. Figure 3.8 shows air temperature differences for the same simulation settings.

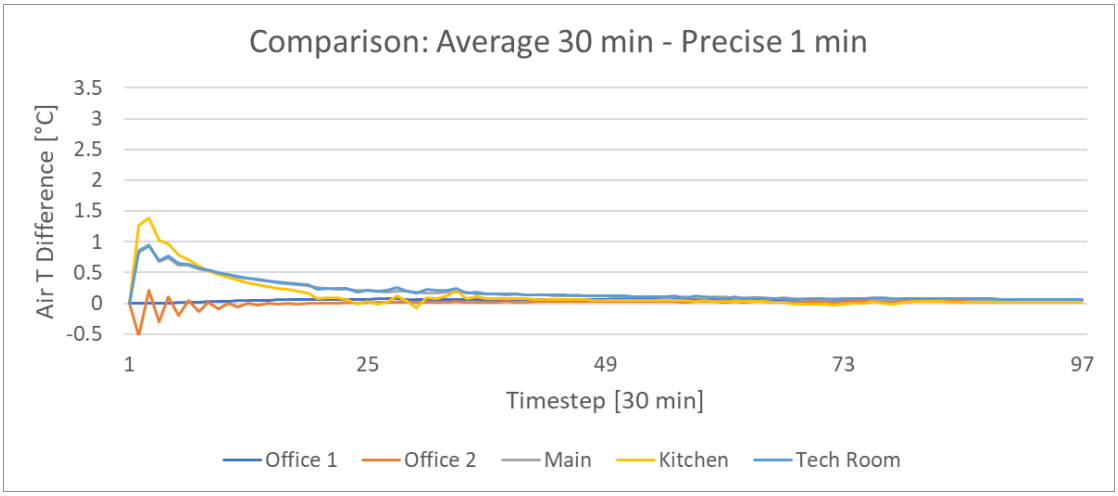

Figure 3.8: Air temperature differences between the vertically averaged model with a 30 min timestep and the precise model with a 1 min timestep.

Air temperature differences are smaller than surface temperature differences, as the change in model configuration happens inside the TABS model, which only slowly affects air nodes. Additionally, transient behavior of the TABS have almost no effect on air temperatures. To find out if the small difference between the two models come from averaging layers or increasing timestep, further simulations are made. Figure 3.9 shows TABS surface temperature differences by comparing the average model with 1 min timestep to the precise model with 1 min timestep, called Simulation Case 2. It is evident that temperature differences are much smaller than before.

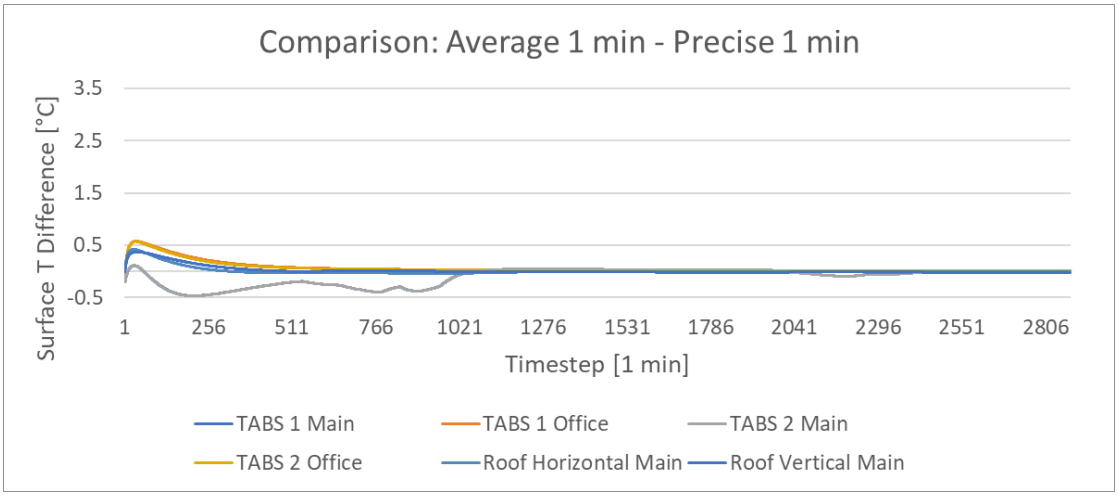

Figure 3.9: TABS surface temperature differences between the vertically averaged model with a 1 min timestep and the precise model with a 1 min timestep.

Air temperatures, presented in Figure 3.10, again show even smaller differences.

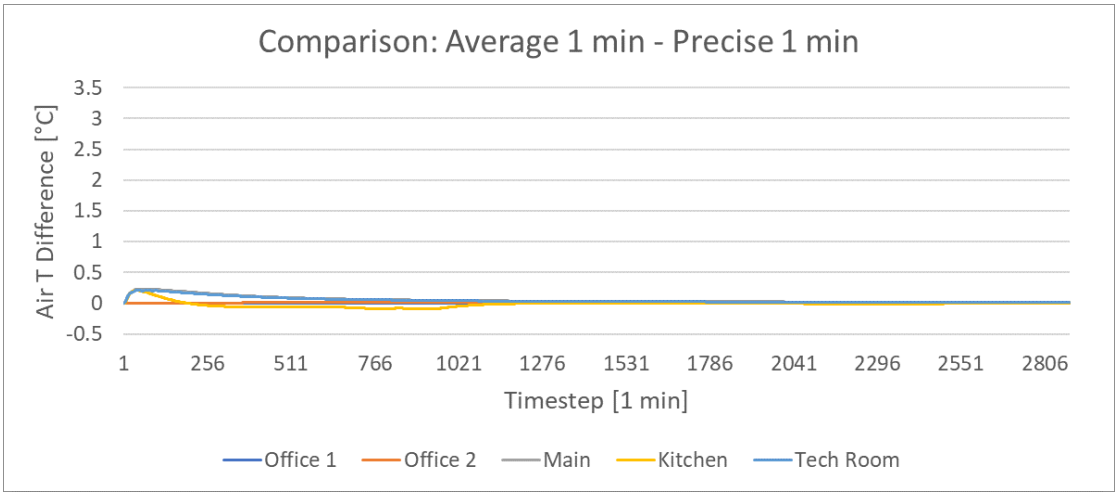

Figure 3.10: Air temperature differences between the vertically averaged model with a 1 min timestep and the precise model with a 1 min timestep.

The bigger part of the difference in Simulation Case 1 must come from somewhere else, which is expected to be due to increasing timestep. Therefore, a third simulation is done by comparing the average model with a 30 min timestep to the average model with a 1 min timestep, called Simulation Case 3, shown in Figure 3.11 and Figure 3.12.

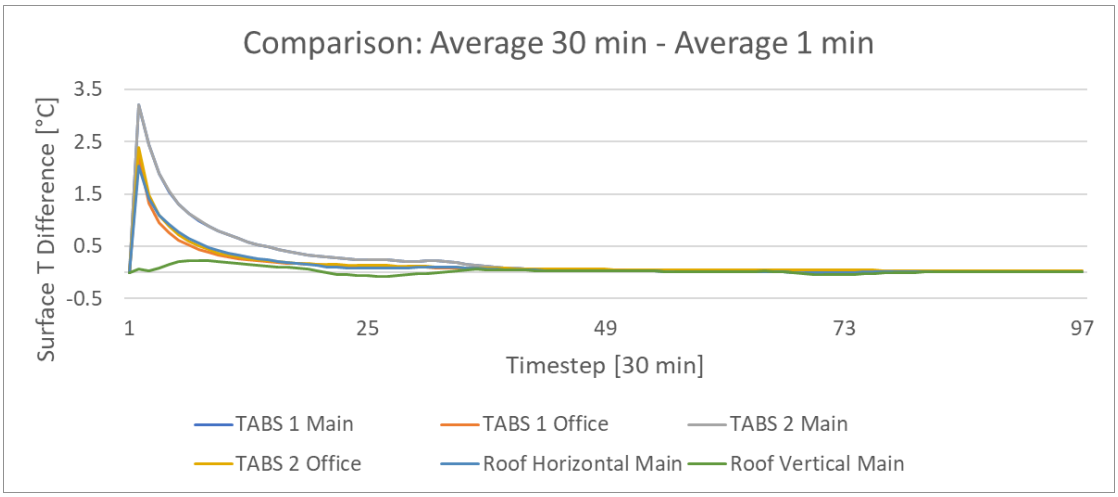

Figure 3.11: TABS surface temperature differences between the vertically averaged model with a 30 min timestep and the averaged model with a 1 min timestep.

As expected, the bigger part of the difference in Simulation Case 1 stems from Simulation Case 3 by increasing timestep. Thus, a vertical layer averaging process is justified,

as the loss of precision comes from the necessary increase in timestep, which further can be neglected as it is relatively small.

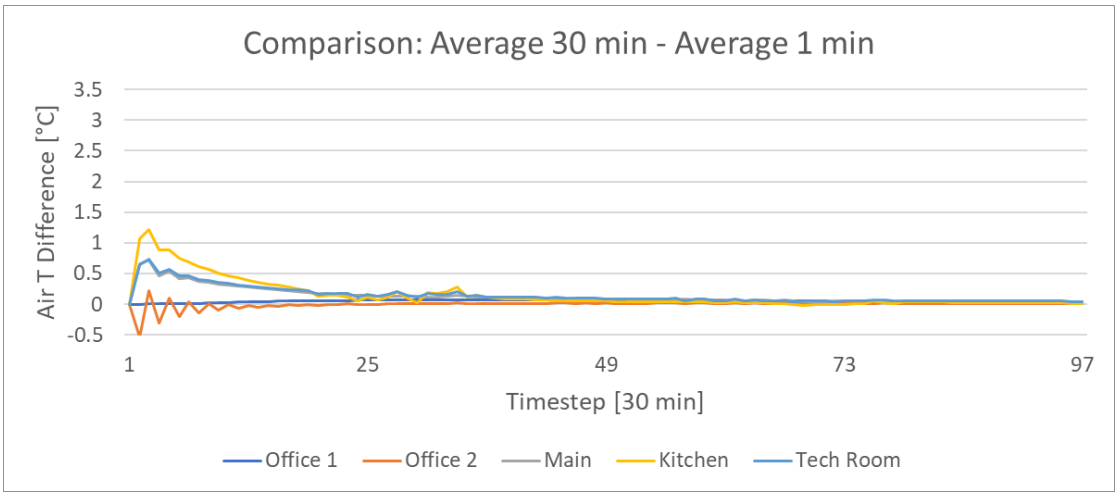

Figure 3.12: Air temperature differences between the vertically averaged model with a 30 min timestep and the averaged model with a 1 min timestep.

3.6 Simplification of Horizontal Subsection Resolution

TABS resolution in the horizontal plane is varied through the number of subsections each loop is defined through. The more subsections per loop, the higher its resolution. HiLo's roof TABS are defined by four subsections and its floor TABS by three, which can be easily changed in MATLAB's Excel input file. Said resolution is compared to a resolution of one subsection per loop for all TABS. Parameters like floor area A_{fl}, activated floor area A_{ta}, pipe length l_p and edge length l_e are summed up, whereas slope angle α and the one varying layer thickness d_{var} are weighted averaged by floor area A_{fl}. A simulation of 48 hours of both the horizontally averaged and precise model is conducted. Frequent transient behavior is included by having TABS in an on state between midnight and 08.00 o'clock in the morning and otherwise off. Figure 3.13 shows surface temperature differences between the two models.

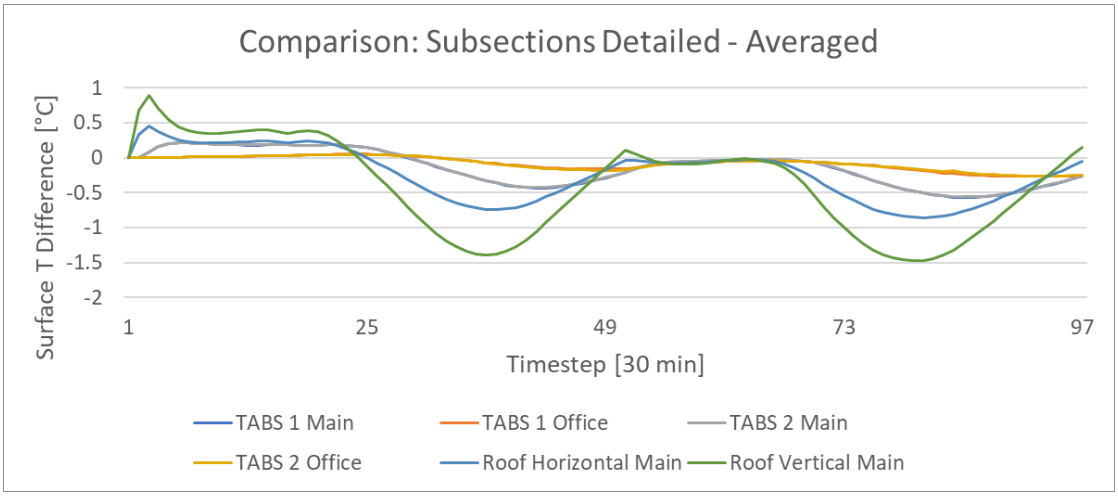

Figure 3.13: TABS surface temperature differences between the horizontally averaged and precise model with a timestep of 30 min.

Bigger differences are visible during switching of the TABS than in stationary operation. Additionally, after model initialization in the first quarter of the simulation, temperature differences do not seem to minimize over time, as was observed in the simplification of vertical layer resolution in Section 3.5. Air temperature differences are shown in Figure 3.14.

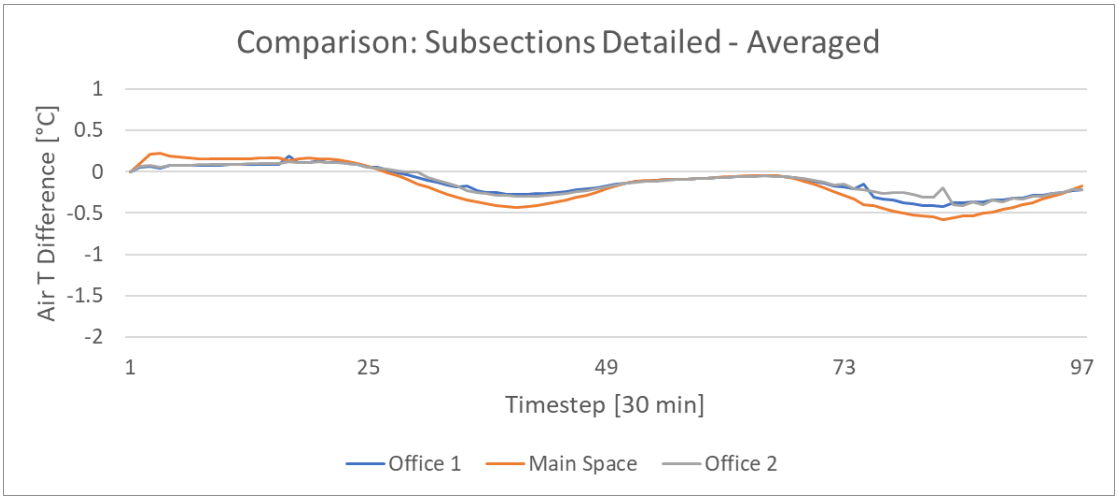

Figure 3.14: Air temperature differences between the horizontally averaged and precise model with a timestep of 30 min.

Again, as air nodes react slower to TABS activity, differences are smaller. In conclusion, general temperature differences are small, but not as small as compared to the vertical layer simplification process in Section 3.5, where a clear statement can be made.

In conclusion, a horizontal layer resolution simplification can only be relatively justified, depending on the models requirements for its level of precision.

3.7 Test Case Night Cooling

In order to test the model and the interaction of its thermal systems, a test case simulation of night cooling is set up. A hot period in mid August is chosen and the model is run for 80 hours. The first 72 hours HiLo is heated up as natural and mechanical ventilation as well as TABS cooling are completely turned off. An occupancy rate of 4 people and 4 PCs in Office 1, 6 people in Main Space and 10 people in Office 2 (conference room) is set to achieve high heat gains. After 72 hours at midnight, each system is turned on, in a separate simulation, to cool down HiLo overnight. Figure 3.15 shows air temperature levels in HiLo's main space for each cooling case. TABS active cooling has the slowest impact on room air, as the thermal energy first has to go through the TABS' slab. Evidently, mechanical ventilation is fastest in changing air temperatures, with natural ventilation behind.

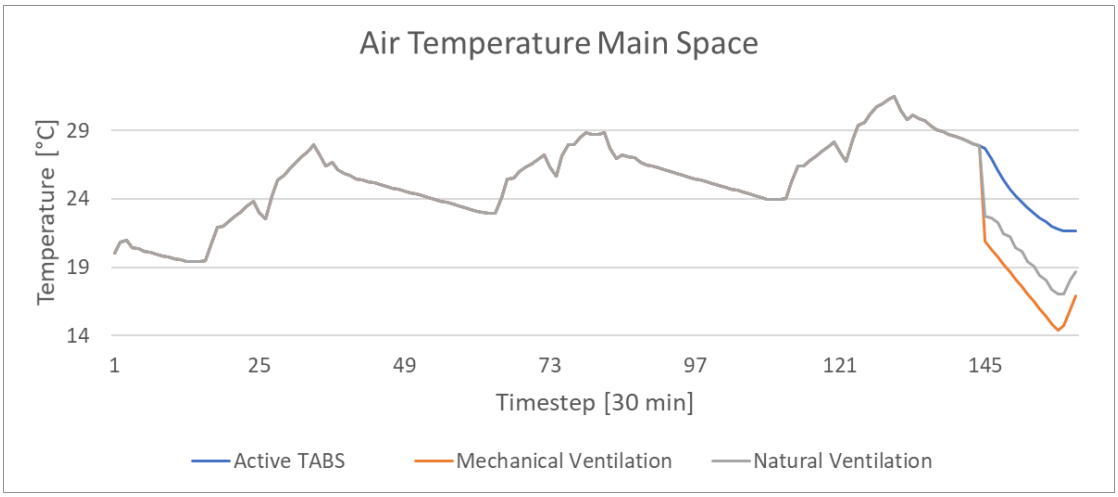

Figure 3.15: Test Case Night Cooling: Air temperatures of main space with natural and mechanical ventilation and TABS active cooling.

Figure 3.16 presents operative temperatures in HiLo's Main Space. When comparing this to Figure 3.15, no significant difference can be seen for active TABS cooling. However, air temperatures for natural and mechanical ventilation are lower than operative temperatures. This is to be expected when ventilating at night, as operative temperature depends on air speed, air temperature and mean radiant temperature [38].

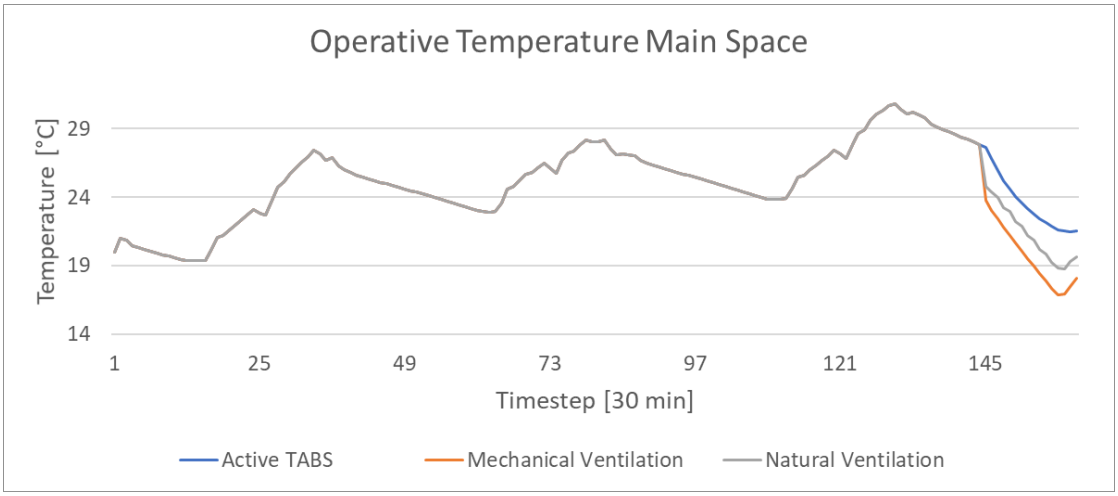

Figure 3.16: Test Case Night Cooling: Operative temperatures of Main Space with natural and mechanical ventilation and TABS active cooling.

Lastly, core temperatures of HiLo's roof TABS are shown in Figure 3.17. As expected, TABS active cooling has the biggest effect on core temperature, as change in thermal energy happens close. Mechanical ventilation comes in second, with natural ventilation on third place having a slightly weaker influence on core temperature.

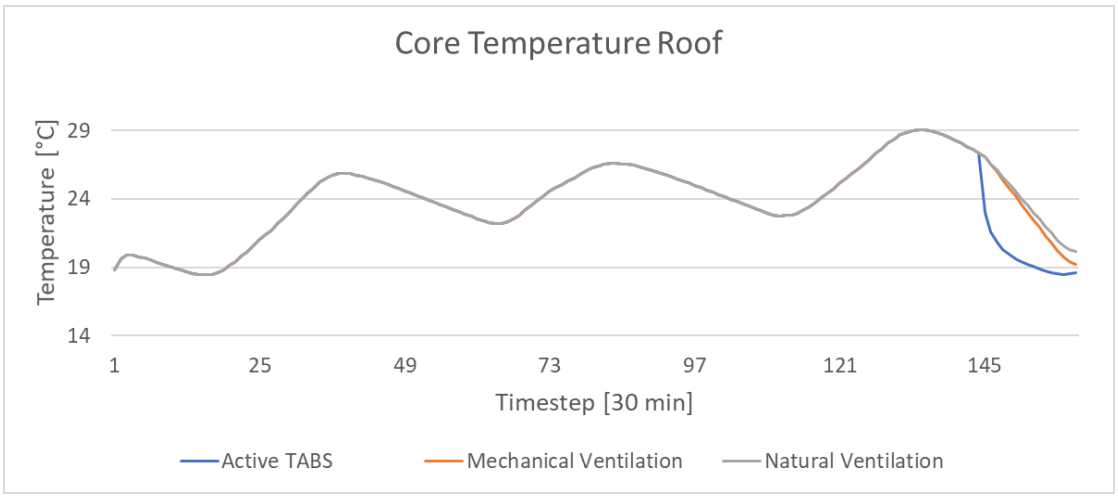

Figure 3.17: Test Case Night Cooling: Core temperatures of Main Space with natural and mechanical ventilation and TABS active cooling.

An interesting observation presents itself when comparing natural with mechanical ventilation. Figure 3.18 shows TABS surface temperatures of the roof in Main Space and TABS 1 in Office 1 for mechanical and natural ventilation.

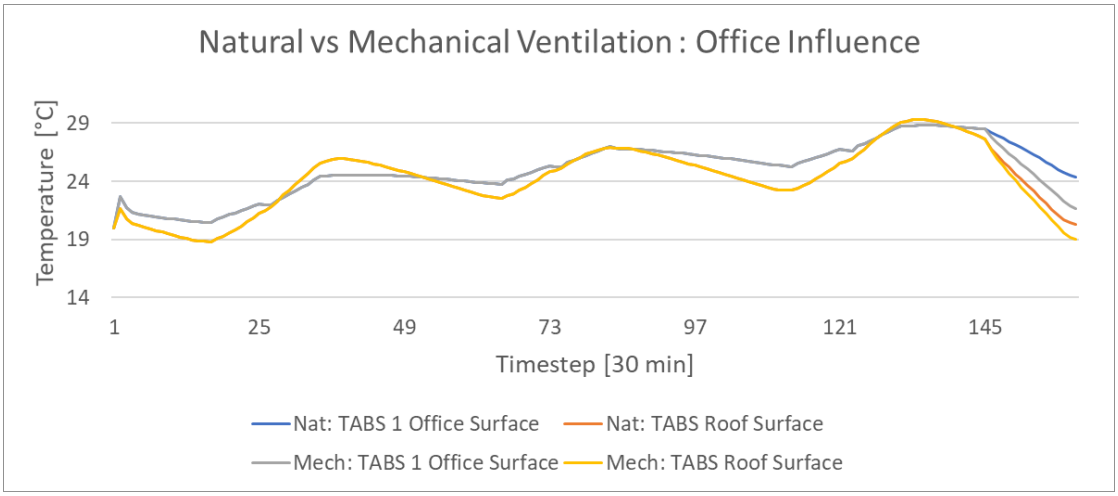

Figure 3.18: Test Case Night Cooling: Mechanical and natural ventilation influence on office temperatures.

By comparing roof surface temperatures for both cases, a small difference can be seen. At the same time, when looking at TABS 1 surface temperatures for both cases, a bigger difference is present. This is due to natural ventilation openings only being available in HiLo's main space. Therefore, both offices are only connected to the natural ventilation system through their doors to Main Space. If windows in offices would be integrated in natural ventilation, the assumption stands that it would have a greater effect on office TABS. This could lead to an overall increase in natural ventilation efficiency and would be worthwhile to investigate.

Conclusion and Outlook

In this master's thesis, the creation of a thermal building model for HiLo is pursued using MATLAB, CONTAM and TRNSYS in combination. An interconnectivity concept to enable an interface between the software programs is established.

A standard TABS model from literature is taken and adjusted to HiLo's exotic specifications for a light weight floor and a thin shell roof. A justified vertical layer simplification process is used to increase time step and decrease nodal temperature matrix complexity, which both shortens computation time from 10 hours to 40 minutes for a 3 day simulation. An additional horizontal layer simplification is tested but can not be justified as absolutely appropriate, since it depends on the users preference on model precision. The TABS model is implemented into TRNSYS and its boundaries are necessarily extended for the roof part.

A ventilation model is created using CONTAM and coupled with TRNSYS. Electrochromic glass in HiLo's facade is included through TRNBuild and a 3D building model is created in SketchUp. To control the above mentioned systems, a gateway through MATLAB is enabled, where in a later stage control algorithms can be implemented.

First test simulations are carried out, which show a correct interaction between all systems. It is found that natural ventilation has a weak effect in office rooms. A possible reason could be because all window openings are located in Main Space, where the only connection to Office 1 and 2 is through their doors. The assumption is made, that it could be worthwhile to further investigate direct integration of natural ventilation into office rooms.

Future work could focus on a validation of the TABS model through CFD comparison study. Additionally, values for building leakages in the CONTAM model should be adjusted after a building pressurization test. Also, a heat recovery component for the research AHU should be added into the TRNSYS model. Realistic values for pressure drops in all heat recoveries should be included. Furthermore, finetuning of interzonal flows and timestep in order to include ventilation in Kitchen and Technical Room has to be done. Finally, the model could be further optimized for speed in general.

Appendix

A.1 MATLAB Code Surface Heat Flux Layer Cases

Depending on vertical layer configuration, heat fluxes from TABS to surface layer can differ. The following figures should help to better understand the calculations in the MATLAB code. Temperature nodes are numbered from top to bottom, meaning top surface layer is number 1 and bottom surface layer is number "numLayers", as defined in the MATLAB code. TABS heat flux to surface calculations for configurations with two layers between core and a specific surface are also valid for configurations of more than two layers between the two nodes.

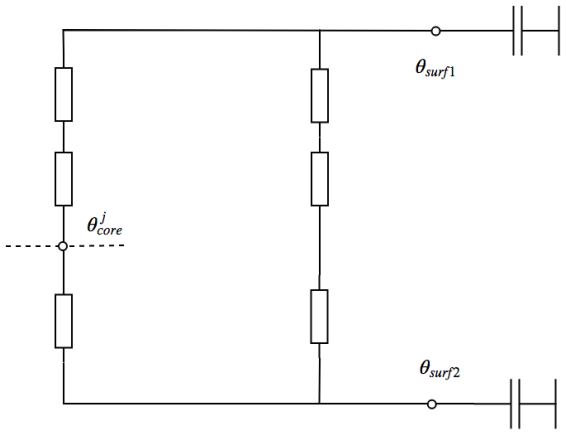

Figure A.1: TABS heat flux calculations to surface RC model Case 1.

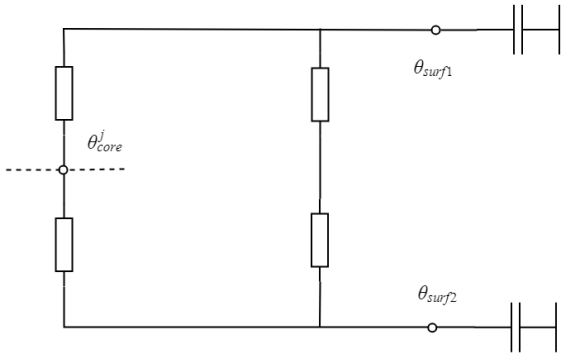

Figure A.2: TABS heat flux calculations to surface RC model Case 2.

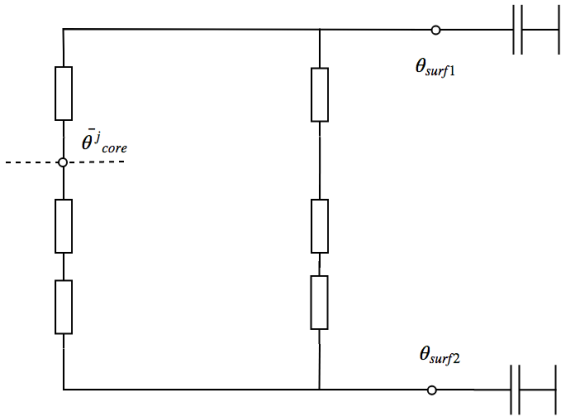

Figure A.3: TABS heat flux calculations to surface RC model Case 3.

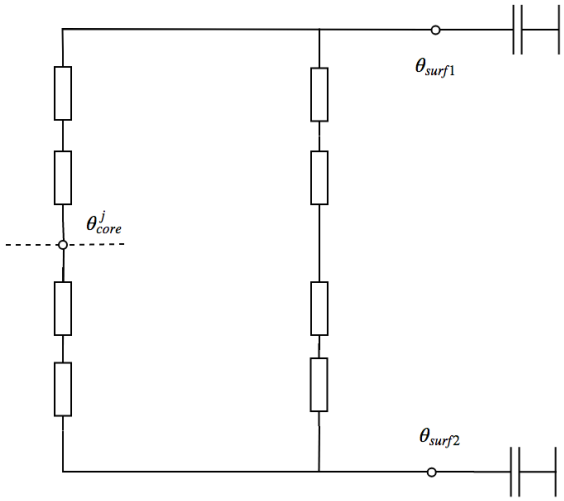

Figure A.4: TABS heat flux calculations to surface RC model Case 4.

A.2 Guide for set up creation

Following, the coupling processes of TRNSYS with MATLAB and CONTAM (including Trnsys3D in SketchUp) are presented. The mentioned files can be found in the "Setup Files" folder.

A.2.1 TRNSYS - MATLAB

This is a short summary of how to set up the TRNSYS - MATLAB connection.

1. Download MATLAB 2014a (the connection only works with 32-Bit versions and this is the latest supported one)
2. Put this versions "...\bin\win32" folder on windows search path
   - 'Windows Control Panel' > 'System and Security' > 'System' > 'Advanced System Settings' > 'Environment variables' > 'System Dialogue' > 'Path' > 'Edit'
   - Add MATLAB's "...\bin\win32" location
3. Add correct Type155.dll to TRNSYS dll folder
   - Go to "...\Trnsys17\Exe\DLLs" and choose the one for MATLAB 2014a
   - Copy the Type155.dll into the folder "...\Trnsys17\Exe"

For more information on TRNSYS - MATLAB coupling, it is advised to visit the cited sources [39][40].

A.2.2 TRNSYS - CONTAM

This is a short summary of how to set up the TRNSYS - CONTAM connection.

1. Make sure TRNSYS version 17.02.0005 or higher is installed
2. Copy "Type98_t17_c3203.dll" to the directory "...\Trnsys17\Userlib\ReleaseDLLs"
3. Copy "ContamX3.exe" to the directory "...\Trnsys17\Exe"
4. When opening a finished model without having done the full coupling process for creating a model, copy the right "*_T3D_coupled.tmf" proforma to "...\Trnsys17 \Studio\Proformas\Utility\Calling External Programs\CONTAM"

For a full project creation refer to the coupling method in the CONTAM documentation [32]. Additionally, one can join the CONTAM Yahoo user group for more tutorial files, updates and help.

A.2.3 TRNSYS - SketchUp

This is a short summary of how to set up the TRNSYS - SketchUp connection.

1. SketchUp 7.0 or higher is required

2. Download Trnsys3d plugin from the cited source and install [41]
3. When opening SketchUp with TRNSYS 17 use "NewFileTemplate˙Trnsys17.idf"

A.3 Tipps and Tricks

A.3.1 Changing Simulation Settings in Coupled Simulation

To switch between .m files of averaged or precise layer configuration, change MATLAB's Type 155 file path to the correct .m file. It is located in its component on the "Special cards" tab and not on "External files", as would be expected. Additionally, time step has to be adjusted as well. Make sure Timestep is changed in TRNSYS' control cards on the left task bar. To change timestep in CONTAM, go to "Simulation">"Set simulation parameters" and adjust all three timestep values.

A.3.2 TRNSYS

1. When cleaning up project files, only the following files are necessary for the model, the rest are created during simulation: TRNSYS deck file .tpf, TRNBuild coupled building file .b17, CONTAM project files .prj and .vef, MATLAB script file .m, EXCEL input file .xlsx
2. When adding new components to the deck file (especially output to file components) and the following error occurs: *"An ASSIGNED logical unit number is already in use, either by the TRNSYS kernal or by a Type"*
    - Change components logical unit to something higher than 42 (unlock the parameter first)

A.3.3 MATLAB

1. Set in Type 155 "Keep Matlab open after simulation" so that a command line from MATLAB will stay open and its workspace is still available, which is good for debugging
2. When editing code in MATLAB coupled with TRNSYS, it is advised to first create a standalone file with fake inputs, which would be supplied by TRNSYS in coupled simulation

A.3.4 CONTAM

1. When creating a new model
    - Check its geometry in SketchUp, as positioning errors can happen
    - When geometry needs to be changed in SketchUp:

- Make two folders with same .prj file in each
- Do full coupling process without changing geometry first with first file, this gives you a correctly coupled .b17 file
- Do coupling process with changing geometry in SketchUp with second file, geometry can be completely changed but it is necessary to keep the zones in their corresponding thermal zones in the T3D .inf file
- Edit second .b17 file with help of first .b17 file (copy paste coupling flows if necessary, set adjacent walls to adjacent, set boundary walls)

2. Air flow paths between zones that already had connecting air flow paths can be created after coupling is done
3. Controls can also be added after the coupling process, in both cases the following procedure should be done:
   - Make full backup of project
   - Modify .prj with new controls and/or air flows
   - In CONTAM: Perform simulation > building check, this will correctly sequence controls
   - Use coupler to generate new .vef and .tmf files
   - Copy .tmf proforma to "...\Trnsys17 \Studio\Proformas\Utility\Calling External Programs\CONTAM"
   - In TRNSYS click on Type 98 > replace and choose new .tmf file

A.3.5 SketchUp

1. Make sure to always edit in Trnsys3d zone by double clicking on object (grey-dashed frame appears)
2. Make sure to save T3D file as .idf file through the T3D task bar
3. It is advised to turn off autosave, as the undo function through Trnsys3d is limited

Bibliography

[1] Gwerder Tödtli, Renggli Lehmann, and Dorer. *TABS Control*. EMPA, 2009.

[2] G. P. Lydon, J. Hofer, B. Svetozarevic, Z. Nagy, and A. Schlueter. Coupling energy systems with lightweight structures for a net plus energy building. *Applied Energy*, 189:310–326, 2017. ISSN 03062619. doi: 10.1016/j.apenergy.2016.11.110. URL http://dx.doi.org/10.1016/j.apenergy.2016.11.110.

[3] NASA. Climate change: How do we know?, 2018. URL https://climate.nasa.gov/evidence/.

[4] NASA. A blanket around the earth, 2018. URL https://climate.nasa.gov/causes/.

[5] European Commission. Roadmap for moving to a low-carbon economy in 2050, 2011.

[6] EPA. Sources of greenhouse gas emissions, 2018. URL https://www.epa.gov/ghgemissions/sources-greenhouse-gas-emissions.

[7] International Energy Agency. Transition to Sustainable Buildings, 2013.

[8] European Commission. Energy Performance of Buildings Directive (recast) 2010/31/EU (EPBD), 2010.

[9] European Union. Directive 2009/28/EC, 2010.

[10] International Energy Agency. Energy Efficiency Requirements in Building Codes Energy Efficiency Policies for New Buildings, 2008.

[11] B V Venkatarama Reddy and K S Jagadish. ScienceDirect - Energy and Buildings : Embodied energy of common and alternative building materials and technologies. 35:129–137, 2003. URL http://www.sciencedirect.com.ezproxy2.library.arizona.edu/science?{_}ob=ArticleURL{&}{_}udi=B6V2V-44TV9S8-1{&}{_}user=9555371{&}{_}coverDate=02/28/2003{&}{_}alid=1744097108{&}{_}rdoc=3{&}{_}fmt=high{&}{_}orig=mlkt{&}{_}origin=mlkt{&}{_}zone=rslt{_}list{_}item{&}{_}cdi=5712{&}{_}sort=v{&}{_}st=17{&}{_}docanchor={&}.

[12] I. Sartori and A. G. Hestnes. Energy use in the life cycle of conventional and low-energy buildings: A review article. *Energy and Buildings*, 39(3):249–257, 2007. ISSN 03787788. doi: 10.1016/j.enbuild.2006.07.001.

[13] SEL, University of Wisconsin USA. Trnsys 17. URL http://www.trnsys.com/.

[14] MathWorks. Matlab. URL https://www.mathworks.com/products/matlab.html.

[15] National Institute of Standards and Technology. Contam. URL https://www.nist.gov/services-resources/software/contam.

[16] B. Lehmann, D. Gyalistras, M. Gwerder, K. Wirth, and S. Carl. Intermediate complexity model for Model Predictive Control of Integrated Room Automation. *Energy and Buildings*, 58:250–262, 2013. ISSN 03787788. doi: 10.1016/j.enbuild.2012.12.007. URL http://dx.doi.org/10.1016/j.enbuild.2012.12.007.

[17] P. Block, A. Schlueter, D. Veenendaal, J. Bakker, M. Begle, I. Hischier, J. Hofer, P. Jayathissa, I. Maxwell, T. Méndez Echenagucia, Z. Nagy, D. Pigram, B. Svetozarevic, R. Torsing, J. Verbeek, A. Willmann, and G. P. Lydon. NEST HiLo: Investigating lightweight construction and adaptive energy systems. *Journal of Building Engineering*, 12(March 2016):332–341, 2017. ISSN 23527102. doi: 10.1016/j.jobe.2017.06.013. URL http://dx.doi.org/10.1016/j.jobe.2017.06.013.

[18] M. Gwerder, B. Lehmann, J. Tödtli, V. Dorer, and F. Renggli. Control of thermally-activated building systems (TABS). *Applied Energy*, 85(7):565–581, 2008. ISSN 03062619. doi: 10.1016/j.apenergy.2007.08.001.

[19] Frauke Oldewurtel, Alessandra Parisio, Colin N. Jones, Dimitrios Gyalistras, Markus Gwerder, Vanessa Stauch, Beat Lehmann, and Manfred Morari. Use of model predictive control and weather forecasts for energy efficient building climate control. *Energy and Buildings*, 45:15–27, 2012. ISSN 03787788. doi: 10.1016/j.enbuild.2011.09.022. URL http://dx.doi.org/10.1016/j.enbuild.2011.09.022.

[20] Martin W Liddament and Agence internationale de l'énergie. Air Infiltration. *A guide to energy efficient ventilation*. Air Infiltration and Ventilation Centre Coventry, 1996.

[21] Tine S. Larsen and Per Heiselberg. Single-sided natural ventilation driven by wind pressure and temperature difference. *Energy and Buildings*, 40(6):1031–1040, 2008. ISSN 03787788. doi: 10.1016/j.enbuild.2006.07.012.

[22] Yi Jiang, Donald Kneale Alexander, Huw Geraint Jenkins, Rob Arthur, and Qingyan Chen. Natural ventilation in buildings: measurement in a wind tunnel and numerical simulation with large eddy simulation. 91:331–353, 2003. ISSN 01676105. doi: 10.1016/S0167-6105(02)00380-X. URL http://orca.cf.ac.uk/2171/.

[23] Nyuk Hien Wong and Sani Heryanto. The study of active stack effect to enhance natural ventilation using wind tunnel and computational fluid dynamics (CFD)

simulations. *Energy and Buildings*, 36(7):668–678, 2004. ISSN 03787788. doi: 10.1016/j.enbuild.2004.01.013.

[24] designingbuildings.co.uk. Mechanical ventilation of buildings, 2018. URL https://www.designingbuildings.co.uk/wiki/Mechanical_ventilation_of_buildings.

[25] breathingbuildings.com. What is hybrid ventilation?, 2018. URL https://www.breathingbuildings.com/knowledge/hybrid-ventilation/.

[26] Hyunjae Chang, Shinsuke Kato, and Tomoyuki Chikamoto. Effects of outdoor air conditions on hybrid air conditioning based on task/ambient strategy with natural and mechanical ventilation in office buildings. *Building and Environment*, 39(2): 153–164, 2004. ISSN 03601323. doi: 10.1016/j.buildenv.2003.07.008.

[27] C. M. Lampert. Large-area smart glass and integrated photovoltaics. *Solar Energy Materials and Solar Cells*, 76(4):489–499, 2003. ISSN 09270248. doi: 10.1016/S0927-0248(02)00259-3.

[28] Carl M. Lampert. Chromogenic switchable glazing: Towards the development of the smart window. *Window Innovations '95*, 16(June):1–19, 1995. URL btech.lbl.gov/papers/37766.pdf.

[29] Carl M Lampert. Optical Switching Technology for Glazing. *Thin Solid Films*, 236 (2-Jan):6–13, 1993. doi: 10.1016/0040-6090(93)90633-Z.

[30] Abdelsalam Aldawoud. Conventional fixed shading devices in comparison to an electrochromic glazing system in hot, dry climate. *Energy and Buildings*, 59:104–110, 2013. ISSN 03787788. doi: 10.1016/j.enbuild.2012.12.031. URL http://dx.doi.org/10.1016/j.enbuild.2012.12.031.

[31] Markus Koschenz and Beat Lehmann. *Thermoaktive Bauteilsysteme tabs: Projekt im Rahmen des Forschungsprogrammes "Rationelle Energienutzung in Gebäuden"*. EMPA, 2000.

[32] Dols William S. *CONTAM Documentation*. NIST, 2000.

[33] G P Lydon, J Hofer, Z Nagy, and A Schlueter. Thermal analysis of a multifunctional floor element. 2015.

[34] Kyu Nam Rhee and Kwang Woo Kim. A 50 year review of basic and applied research in radiant heating and cooling systems for the built environment. *Building and Environment*, 91:166–190, 2015. ISSN 03601323. doi: 10.1016/j.buildenv.2015.03.040. URL http://dx.doi.org/10.1016/j.buildenv.2015.03.040.

[35] Thijs Defraeye, Bert Blocken, and Jan Carmeliet. Convective heat transfer coefficients for exterior building surfaces: Existing correlations and CFD modelling. *Energy Conversion and Management*, 52(1):512–522, 2011. ISSN 01968904. doi: 10.1016/j.enconman.2010.07.026.

[36] Andrew K. Persily, Elizabeth M. Ivy. Input Data for Multizone Airflow and IAQ Analysis, 2000. URL https://www.nist.gov/el/energy-and-environment-division-73200/nist-multizone-modeling/software-tools/contam/libraries.

[37] David Lorenzetti. Trnflow and relative humidity, 2006. URL https://www.mail-archive.com/trnsys-users@engr.wisc.edu/msg00524.html.

[38] designingbuildings.co.uk. Operative temperature, 2018. URL https://www.designingbuildings.co.uk/wiki/Operative_temperature.

[39] Michael Kummert. Type 155: Trnsys-matlab link, 2003. URL http://sel.me.wisc.edu/trnsys/trnlib/trnsys-matlab/type155-manual.html.

[40] Michael Kummert. Trnsys - matlab link example, 2003. URL http://sel.me.wisc.edu/trnsys/trnlib/trnsys-matlab/trnsys-matlab-example.html.

[41] TRANSSOLAR. Trnsys3d - free plugin for sketchup, 2018. URL http://trnsys.de/docs/trnsys3d/trnsys3d_uebersicht_en.htm.